





A Consistent Set of Empirical Scaling Relations for Spiral Galaxies: The $(v_{\max}, M_{\text{DM}})-(\sigma_0, M_{\text{BH}}, \phi)$ Relations

Benjamin L. Davis¹ , Alister W. Graham¹ , and Françoise Combes^{2,3} 

¹ Centre for Astrophysics and Supercomputing, Swinburne University of Technology, Hawthorn, VIC 3122, Australia; benjamindavis@swin.edu.au

² Observatoire de Paris, LERMA, CNRS, PSL Université, Sorbonne Université, F-75014 Paris, France

³ Collège de France, 11 Place Marcelin Berthelot, F-75005 Paris, France

Received 2019 January 19; revised 2019 April 4; accepted 2019 April 16; published 2019 May 24

Abstract

Using the latest sample of 48 spiral galaxies having a directly measured supermassive black hole mass, M_{BH} , we determine how the maximum disk rotational velocity, v_{\max} (and the implied dark matter halo mass, M_{DM}), correlates with the (i) black hole mass, (ii) central velocity dispersion, σ_0 , and (iii) spiral-arm pitch angle, ϕ . We find that $M_{\text{BH}} \propto v_{\max}^{10.62 \pm 1.37} \propto M_{\text{DM}}^{4.35 \pm 0.66}$, significantly steeper than previously reported, and with a total root mean square scatter (0.58 dex) similar to that about the $M_{\text{BH}}-\sigma_0$ relation for spiral galaxies—in stark disagreement with claims that M_{BH} does not correlate with disks. Moreover, this $M_{\text{BH}}-v_{\max}$ relation is consistent with the unification of the Tully–Fisher relation (involving the total stellar mass, $M_{\ast,\text{tot}}$) and the steep $M_{\text{BH}} \propto M_{\ast,\text{tot}}^{3.05 \pm 0.53}$ relation observed in spiral galaxies. We also find that $\sigma_0 \propto v_{\max}^{1.55 \pm 0.25} \propto M_{\text{DM}}^{0.63 \pm 0.11}$, consistent with past studies connecting stellar bulges (with $\sigma_0 \gtrsim 100 \text{ km s}^{-1}$), dark matter halos, and a nonconstant v_{\max}/σ_0 ratio. Finally, we report that $\tan|\phi| \propto (-1.18 \pm 0.19) \log v_{\max} \propto (-0.48 \pm 0.09) \log M_{\text{DM}}$, providing a novel formulation between the geometry (i.e., the logarithmic spiral-arm pitch angle) and kinematics of spiral galaxy disks. While the $v_{\max}-\phi$ relation may facilitate distance estimations to face-on spiral galaxies through the Tully–Fisher relation and using ϕ as a proxy for v_{\max} , the $M_{\text{DM}}-\phi$ relation provides a path for determining dark matter halo masses from imaging data alone. Furthermore, based on a spiral galaxy sample size that is double the size used previously, the self-consistent relations presented here provide dramatically revised constraints for theory and simulations.

Key words: black hole physics – dark matter – galaxies: evolution – galaxies: fundamental parameters – galaxies: spiral – galaxies: structure

1. Introduction

Building on the possibility of unseen mass in the solar neighborhood (Jeans 1922; Kapteyn 1922; Lindblad 1926; Oort 1932), dark matter has been considered by many astronomers to be prevalent in galaxy clusters since the 1930s (Zwicky 1933; Smith 1936; Zwicky 1937; Schwarzschild 1954; Rood 1965). In addition, the study of galaxy rotation curves provided strong evidence for the existence of dark matter (Babcock 1939; Oort 1940; Freeman 1970; Rubin & Ford 1970; Rogstad & Shostak 1972; Roberts & Rots 1973; Rubin et al. 1977, 1978; Krumm & Salpeter 1979; Rubin et al. 1980; Bosma 1981; Persic & Salucci 1988; Broeils 1992). The notion of nonbaryonic dark matter subsequently grew as a mechanism to explain this anomalous gravitational phenomenon (Gershtein & Zel’dovich 1966; Marx & Szalay 1972; Cowsik & McClelland 1972; Szalay & Marx 1976). Intriguingly, dark matter is believed to account for $84\% \pm 1\%$ of the total mass in the universe (Planck Collaboration et al. 2018), but it remains elusive despite considerable efforts to achieve direct instrumental detection of its theorized particles (e.g., Tan et al. 2016; Akerib et al. 2017; Aprile et al. 2018).⁴ The concept of supermassive black holes (SMBHs) lurking in the center of galaxies has also had an interesting history of study (see Kormendy & Richstone 1995; Longair 1996, 2006; Ferrarese & Ford 2005, for reviews on SMBHs). It was in a spiral galaxy, our Milky Way, where an SMBH (Sagittarius A^{*}) was first calculated to exist (Lynden-Bell 1969; Sanders & Lowinger 1972). For half a century, confidence in its existence gradually increased from suggestion to certainty (see Alexander 2005 and Genzel et al. 2010

for reviews on Sagittarius A^{*}), with modern measurements (Gravity Collaboration et al. 2018a, 2018b; Amorim et al. 2019) even detecting the effects of general relativity (Einstein 1916; Schwarzschild 1916; Kerr 1963; Bardeen et al. 1972) in its vicinity, and providing direct imaging via very long baseline interferometry (Issaoun et al. 2019).⁵ In contrast to dark matter, SMBHs residing at the centers of galaxies are thought to constitute a tiny fraction of the universe’s total mass (Graham et al. 2007; Vika et al. 2009; Davis et al. 2014; Mutlu-Pakdil et al. 2016).

Astronomers have long been comfortable with the idea that SMBH masses (M_{BH}) should correlate with properties of their host galactic bulges, as evidenced by a vast literature dedicated to the study of correlations with a bulge’s stellar velocity dispersion (σ_0), (baryonic and total) mass, stellar luminosity, Sérsic index, etc. (see Graham 2016, for a review), although many theoretical models advocate that the total gravitational mass of a galaxy or its most dominant component, the mass of its dark matter halo (M_{DM}), should dictate the formation of SMBHs (e.g., Loeb & Rasio 1994; Haehnelt et al. 1998; Silk & Rees 1998; Cattaneo et al. 1999; Haehnelt & Kauffmann 2000; Monaco et al. 2000; Adams et al. 2001). The rotation curve informs us about the total mass of a disk galaxy and its dark matter component. Therefore, the rotational velocity profile of a galaxy disk, $v_{\text{rot}}(R)$, can be considered a surrogate⁶ for its M_{DM} .

⁵ See also the revolutionary imaging of the central SMBH in M87 (Event Horizon Telescope Collaboration et al. 2019).

⁶ Globular clusters have also been shown to be apropos tracers of the dark matter halo mass; both the globular cluster system mass (Spitler & Forbes 2009) and the number of globular clusters (Burkert & Forbes 2019) of a galaxy are directly proportional to its dark matter halo mass.

⁴ See Seigar (2015), Arcadi et al. (2018), Hooper (2018), and Salucci (2019) for reviews on searches for dark matter.

Thus, a relation between M_{BH} and some measure of $v_{\text{rot}}(R)$ or M_{DM} should be expected in observational data.

Recently, we showed in Davis et al. (2018) that a significant correlation exists between the total stellar mass ($M_{*,\text{tot}}$) of a spiral galaxy and the mass of its central black hole. When combined with the well-known Tully & Fisher (1977) relation between the total stellar luminosity/mass of a galaxy and its rotational velocity, one obtains a relation between v_{rot} and M_{BH} . A contemporary study by Tiley et al. (2019) has defined the $z \approx 0$ Tully–Fisher relation between $M_{*,\text{tot}}$ and v_{rot} for late-type galaxies⁷ to be such that

$$M_{*,\text{tot}} \propto v_{\text{rot}}^{4.0 \pm 0.1}. \quad (1)$$

In Davis et al. (2018), we found that

$$M_{\text{BH}} \propto M_{*,\text{tot}}^{3.05 \pm 0.53} \quad (2)$$

for spiral galaxies. Therefore, we should expect to find

$$M_{\text{BH}} \propto v_{\text{rot}}^{12.2 \pm 2.1}, \quad (3)$$

which can subsequently be converted into an $M_{\text{BH}}-M_{\text{DM}}$ relation using an expression from Katz et al. (2018b) between v_{rot} and M_{DM} .

In addition to our focus on black hole mass scaling relations for spiral galaxies in this work, we also investigate scaling relations between v_{rot} (and M_{DM}) with both σ_0 and the logarithmic spiral-arm pitch angle (ϕ). A $v_{\text{rot}}-\sigma_0$ ratio or relation for disk galaxies was first suggested by Whitmore et al. (1979) and Whitmore & Kirshner (1981). They found $v_{\text{rot}}/\sigma_0 \sim 1.7$ by measuring HI line widths for local S0 and spiral galaxies. More recently, Cresci et al. (2009) found that gas-rich, turbulent, star-forming $z \sim 2$ disk galaxies exhibit $v_{\text{rot}}/\sigma_0 \sim 4.4$.⁸ The $v_{\text{rot}}-\sigma_0$ relation represents an intriguing connection between the stellar bulge of a galaxy and its dark matter halo, although for spiral galaxies with turbulent disks, σ_0 may trace the stellar disk as much as the bulge. As a result, regular study of the $v_{\text{rot}}-\sigma_0$ relation has persisted for 40 yr. We contribute to this legacy with our refinement of the $v_{\text{rot}}-\sigma_0$ relation and an original quantification of the $M_{\text{DM}}-\sigma_0$ relation based on the $v_{\text{rot}}-M_{\text{DM}}$ expression in Katz et al. (2018b).

As for the connection with the logarithmic spiral-arm pitch angle, Kennicutt (1981) and Kennicutt & Hodge (1982) presented an observational study of the shape of spiral arms and showed that the maximum rotational velocity of a galaxy disk, v_{max} , correlated with the spiral-arm pitch angle. They found a definitive anticorrelation, such that galaxies with higher v_{max} have lower ϕ , i.e., more tightly wound spiral patterns. Their tantalizing empirical result suggests that the trend of shapes across the spiral sequence of galaxies is partly kinematic in origin. We use our measured pitch angle values from Davis et al. (2017) to quantify this $v_{\text{max}}-\phi$ (and $M_{\text{DM}}-\phi$) relation, and compare the scatter with other relations involving ϕ .

In this work, we endeavor to determine scaling relations from our (currently) complete sample of spiral galaxies with directly measured black hole masses. In Section 2 we describe our compilation of σ_0 , v_{max} , M_{BH} , and ϕ measurements and detail our conversion of v_{max} into M_{DM} . Section 3 provides our

regression analyses and discussion for six relations: $v_{\text{rot}}-\sigma_0$, $M_{\text{DM}}-\sigma_0$, $M_{\text{BH}}-v_{\text{rot}}$, $M_{\text{BH}}-M_{\text{DM}}$, $v_{\text{rot}}-\phi$, and $M_{\text{DM}}-\phi$. Finally, Section 4 presents our interpretation of the results and elucidates their significance. All printed uncertainties are 1σ ($\approx 68.3\%$) confidence intervals. All magnitudes are quoted in the Vega system.

2. Data

In Davis et al. (2017), we compiled a comprehensive sample of 44 galaxies classified as spirals and having directly measured (dynamical)⁹ black hole masses (see Table 1). In Davis et al. (2018, 2019), we used this sample to determine how the black hole mass of a spiral galaxy scales with its total stellar and bulge stellar masses, respectively. Here, we use the same sample, plus four new galaxies (NGC 613, NGC 1365, NGC 1566, and NGC 1672) from Combes et al. (2019), making our total sample of spiral galaxies with directly measured black hole masses twice the size of recent studies (e.g., Sabra et al. 2015). For this expanded sample, we tabulate the ϕ and σ_0 measurements (predominantly from Davis et al. 2017), plus the v_{max} measurements that we have assembled from the literature. We use this rotational velocity to draw a connection to the dark matter halo mass, which dictates the maximum rotational velocity at the outer radii of a galaxy. As revealed in Davis et al. (2017), particular care was taken to obtain the fundamental spiral-arm pitch angle rather than the harmonics, which may be a factor of two or three smaller or larger and are accidentally obtained when an insufficiently long section of spiral arms is used.

Forty-two galaxies out of our total sample of 48 galaxies have v_{max} measurements in the literature. These are mostly (29 out of 42) from the HyperLeda database¹⁰ (Paturel et al. 2003), which provides homogenized maximum rotational velocities calculated from the 21 cm line maximum widths (W_{max}) or available rotation curves (generally H α rotation curves). These velocities are derived from the observed line-of-sight velocities (v_{obs}) after correcting for inclination (i), such that

$$v_{\text{max}} = \frac{W_{\text{max}}}{2 \sin(i)} = \frac{v_{\text{obs}}}{\sin(i)}. \quad (4)$$

The internal orbital velocity for a galaxy at a given radius can be used to estimate the mass of the galaxy interior to that radius; this mass is the sum of the baryonic and nonbaryonic (i.e., dark matter) masses. At the outer regions of a galaxy, the gravitational potential is thought to be dominated by the dark matter halo (but see Milgrom 1983 and McGaugh & Schombert 2015), for which the maximum rotational velocity is a proxy.

For our conversions from v_{max} into M_{DM} , we consulted the recent work of Katz et al. (2018b), who determined $M_{\text{DM}}-v_{\text{rot}}$ relations from the *Spitzer* Photometry and Accurate Rotation Curves (SPARC) sample gas and stellar mass models (Lelli et al. 2016) and employed the Markov chain Monte Carlo simulations from Katz et al. (2017) to empirically determine halo masses. Katz et al. (2018b) present evidence that a variety

⁷ If we calculate the Tully–Fisher relation from our data set, we find that $M_{*,\text{tot}} \propto v_{\text{rot}}^{3.94 \pm 1.01}$, which is consistent with Equation (1) at the level of 0.05 σ .

⁸ The dynamics of newly assembled massive objects (DYNAMO) project (Green et al. 2010, 2014; Bassett et al. 2014) demonstrated that their more local ($z \sim 0.1$) sample of galaxies, selected to have high star formation rates, are analogs of turbulent $z \approx 2$ disk galaxies, with similar v_{rot}/σ_0 ratios.

⁹ We include direct, dynamical (not including upper or lower limit) measurements derived from stellar proper motions, stellar dynamics, gas dynamics, or maser emission. We do not include black hole masses estimated via reverberation mapping, which is calibrated to the $M_{\text{BH}}-\sigma_0$ relation (e.g., Onken et al. 2004; Peterson et al. 2004; Graham et al. 2011).

¹⁰ <http://leda.univ-lyon1.fr/>

Table 1
Sample of 48 Spiral Galaxies with Directly Measured Supermassive Black Hole Masses

Galaxy	Bar?	$\log\left(\frac{M_{\text{BH}}}{M_{\odot}}\right)$	$ \phi $ (deg)	σ_0 (km s ⁻¹)	v_{max} (km s ⁻¹)	v_{max} Reference	i (deg)	$\log\left(\frac{M_{\text{DM}}}{M_{\odot}}\right)$
(1)	(2)	(3)	(4)	(5)	(6)	(7)	(8)	(9)
Circinus	✓	$6.25^{+0.10}_{-0.12}$	17.0 ± 3.9	148 ± 18	153 ± 7	Courtois et al. (2009)	66.9	11.66 ± 0.12
Cygnus A ^a	✓	$9.44^{+0.11}_{-0.14}$	2.7 ± 0.2	270 ± 90
ESO 558-G009		$7.26^{+0.03}_{-0.04}$	16.5 ± 1.3	170 ± 20
IC 2560	✓	$6.49^{+0.19}_{-0.21}$	22.4 ± 1.7	141 ± 10	196 ± 3	HyperLeda	65.6	11.92 ± 0.11
J0437+2456	✓	$6.51^{+0.04}_{-0.05}$	16.9 ± 4.1	110 ± 13
Milky Way	✓	6.60 ± 0.02	13.1 ± 0.6	105 ± 20	198 ± 6^b	Eilers et al. (2019)	...	11.94 ± 0.12^c
Mrk 1029		$6.33^{+0.10}_{-0.13}$	17.9 ± 2.1	132 ± 15
NGC 0224	✓	$8.15^{+0.27}_{-0.11}$	8.5 ± 1.3	154 ± 4	257 ± 6	HyperLeda	72.2	12.21 ± 0.12
NGC 0253	✓	7.00 ± 0.30	13.8 ± 2.3	96 ± 18	196 ± 3	HyperLeda	75.3	11.93 ± 0.11
NGC 0613	✓	7.57 ± 0.15^d	15.8 ± 4.3^e	122 ± 18^f	289 ± 5	HyperLeda	35.7	12.34 ± 0.13
NGC 1068	✓	6.75 ± 0.08	17.3 ± 1.9	174 ± 9	192 ± 12	HyperLeda	37.2	11.90 ± 0.13
NGC 1097	✓	$8.38^{+0.03}_{-0.04}$	9.5 ± 1.3	195 ± 5	241 ± 34	HyperLeda	48.4	12.14 ± 0.19
NGC 1300	✓	$7.71^{+0.19}_{-0.14}$	12.7 ± 2.0	218 ± 29	189 ± 28	Mathewson et al. (1992)	49.6	11.88 ± 0.19
NGC 1320		$6.78^{+0.24}_{-0.34}$	19.3 ± 2.0	110 ± 10	183 ± 13	HyperLeda	65.8	11.85 ± 0.13
NGC 1365	✓	6.60 ± 0.30^d	11.4 ± 0.1^e	141 ± 19^f	198 ± 3	HyperLeda	62.6	11.94 ± 0.11
NGC 1398	✓	8.03 ± 0.11	9.7 ± 0.7	196 ± 18	289 ± 7	HyperLeda	47.7	12.33 ± 0.13
NGC 1566	✓	6.83 ± 0.30^d	17.8 ± 3.7^g	98 ± 7^f	154 ± 14	Mathewson & Ford (1996)	47.9	11.67 ± 0.15
NGC 1672	✓	6.70 ± 0.10^d	15.4 ± 3.6^e	111 ± 3^h	213 ± 8	HyperLeda	28.2	12.01 ± 0.12
NGC 2273	✓	6.97 ± 0.09	15.2 ± 3.9	141 ± 8	211 ± 16	HyperLeda	50.1	12.00 ± 0.13
NGC 2748		$7.54^{+0.17}_{-0.25}$	6.8 ± 2.2	96 ± 10	188 ± 27	Erroz-Ferrer et al. (2015)	52.9	11.88 ± 0.19
NGC 2960		$7.06^{+0.16}_{-0.17}$	14.9 ± 1.9	166 ± 16	257 ± 34	HyperLeda	51.5	12.21 ± 0.18
NGC 2974	✓	$8.23^{+0.07}_{-0.08}$	10.5 ± 2.9	232 ± 4	284 ± 26	HyperLeda	48.1	12.32 ± 0.16
NGC 3031	✓	$7.83^{+0.11}_{-0.07}$	13.4 ± 2.3	152 ± 2	237 ± 10	HyperLeda	54.4	12.12 ± 0.13
NGC 3079	✓	$6.38^{+0.11}_{-0.13}$	20.6 ± 3.8	175 ± 12	216 ± 6	HyperLeda	75.0	12.03 ± 0.12
NGC 3227	✓	$7.88^{+0.13}_{-0.14}$	7.7 ± 1.4	127 ± 6	240 ± 10	Haynes et al. (2018)	59.3	12.14 ± 0.13
NGC 3368	✓	$6.89^{+0.08}_{-0.10}$	14.0 ± 1.4	119 ± 4	218 ± 15	HyperLeda	46.2	12.03 ± 0.14
NGC 3393	✓	$7.49^{+0.05}_{-0.16}$	13.1 ± 2.5	197 ± 28	193 ± 48	Courtois et al. (2009)	31.8	11.91 ± 0.28
NGC 3627	✓	6.95 ± 0.05	18.6 ± 2.9	127 ± 6	188 ± 7	HyperLeda	59.2	11.88 ± 0.12
NGC 4151	✓	$7.68^{+0.15}_{-0.58}$	11.8 ± 1.8	116 ± 3^i	272 ± 16	Mundell et al. (1999)	46.7	12.27 ± 0.14
NGC 4258	✓	7.60 ± 0.01	13.2 ± 2.5	133 ± 7	222 ± 8	HyperLeda	63.3	12.05 ± 0.12
NGC 4303	✓	$6.58^{+0.07}_{-0.26}$	14.7 ± 0.9	95 ± 8	214 ± 7	HyperLeda	32.3	12.02 ± 0.12
NGC 4388	✓	6.90 ± 0.11	18.6 ± 2.6	100 ± 10	180 ± 5	HyperLeda	71.6	11.84 ± 0.11
NGC 4395	✓	$5.64^{+0.22}_{-0.12}$	22.7 ± 3.6	27 ± 4	145 ± 11	Haynes et al. (2018)	47.7	11.60 ± 0.14
NGC 4501		7.13 ± 0.08	12.2 ± 3.4	166 ± 7	272 ± 4	HyperLeda	62.9	12.27 ± 0.12
NGC 4594		8.34 ± 0.10	5.2 ± 0.4	226 ± 3	277 ± 22^j	HyperLeda	47.9	12.29 ± 0.15
NGC 4699	✓	$8.34^{+0.13}_{-0.15}$	5.1 ± 0.4	192 ± 9	258 ± 7	HyperLeda	42.6	12.22 ± 0.12
NGC 4736	✓	$6.78^{+0.09}_{-0.11}$	15.0 ± 2.3	107 ± 4	182 ± 5	HyperLeda	31.8	11.84 ± 0.11
NGC 4826		$6.07^{+0.14}_{-0.16}$	24.3 ± 1.5	97 ± 6	167 ± 9	HyperLeda	55.2	11.75 ± 0.12
NGC 4945	✓	6.15 ± 0.30	22.2 ± 3.0	118 ± 18	171 ± 2	HyperLeda	77.0	11.78 ± 0.11
NGC 5055		$8.94^{+0.09}_{-0.11}$	4.1 ± 0.4	101 ± 3	270 ± 14	Flores et al. (1993)	52.5	12.26 ± 0.13
NGC 5495	✓	$7.04^{+0.08}_{-0.09}$	13.3 ± 1.4	166 ± 19	202 ± 43	HyperLeda	32.8	11.96 ± 0.25
NGC 5765b	✓	7.72 ± 0.05	13.5 ± 3.9	162 ± 19	238 ± 15	HyperLeda	49.1	12.13 ± 0.13
NGC 6264	✓	7.51 ± 0.06	7.5 ± 2.7	158 ± 15
NGC 6323	✓	$7.02^{+0.13}_{-0.14}$	11.2 ± 1.3	158 ± 25
NGC 6926	✓	$7.74^{+0.26}_{-0.74}$	9.1 ± 0.7	...	246 ± 10	HyperLeda	78.1	12.16 ± 0.13
NGC 7582	✓	$7.67^{+0.09}_{-0.08}$	10.9 ± 1.6	147 ± 19	200 ± 9	HyperLeda	64.3	11.95 ± 0.12
UGC 3789	✓	7.06 ± 0.05	10.4 ± 1.9	107 ± 12	210 ± 14	HyperLeda	43.2	11.99 ± 0.13
UGC 6093	✓	$7.41^{+0.04}_{-0.03}$	10.2 ± 0.9	155 ± 18	170 ± 59	Haynes et al. (2018)	23.2	11.77 ± 0.38

Notes. Column (1): galaxy name. Column (2): indicates (with a checkmark) whether the galaxy exhibits a barred morphology. Column (3): black hole mass listed in Davis et al. (2017, 2019), compiled from references therein. Column (4): logarithmic spiral-arm pitch angle (face-on, absolute value in degrees) from Davis et al. (2017). Column (5): central ($\lesssim 0.6$ kpc) stellar velocity dispersion listed in Davis et al. (2017), compiled from references therein (HyperLeda values have been updated as of 2018 December). Column (6): maximum rotational velocity of the galaxy disk (Equation (4)). Column (7): reference for maximum rotational velocity. Column (8): inclination angle (from the reference in Column (7), if available) used to correct the observed rotational velocity via Equation (4). Column (9): dark matter halo mass from Equation (5); their errors should be considered minimum estimates due to lack of an intrinsic scatter measurement from Katz et al. (2018b) for Equation (5).

^a Cygnus A has been questionably classified as a spiral galaxy; it resembles a dusty early-type galaxy, although with nuclear spiral arms.

^b The outermost circular velocity (at a Galactocentric radius of 24.82 kpc) from Eilers et al. (2019).

^c Compare with the recent measurement of $\log(M_{\text{DM}}/M_{\odot}) = 11.86 \pm 0.01$ from Eilers et al. (2019) for the Galaxy.

^d Black hole mass derived from dynamical gas measurements by Combes et al. (2019), who report on Atacama Large Millimeter/submillimeter Array observations of molecular tori around active galactic nuclei.

^e New pitch angle measurement using 2DFFT (Davis et al. 2012, 2016), SPIRALITY (Shields et al. 2015a, 2015b), and/or SPARCFIRE (Davis & Hayes 2014) software packages.

^f From the HyperLeda database (Patrel et al. 2003), accessed 2018 December.

^g From Davis et al. (2014).

^h From Garcia-Rissmann et al. (2005).

ⁱ From Onken et al. (2014).

^j Apparent maximum stellar rotation velocity of the disk-like component of this dual morphology galaxy (see Gadotti & Sánchez-Janssen 2012).

of rotational measurements are capable of accurately predicting dark matter halo masses in spiral galaxies. They explored many of the standard measurements: (i) v_{flat} , the rotational velocity along the flat portion of a rotation curve, (ii) $v_{2.2}$, the rotational velocity at 2.2 disk scale lengths, (iii) v_{eff} , the rotational velocity at the effective half-light radius of a galaxy, and (iv) v_{max} . Katz et al. (2018b) presented empirical relations for the $M_{\text{DM}}-v_{\text{flat}}$, $M_{\text{DM}}-v_{2.2}$, $M_{\text{DM}}-v_{\text{eff}}$, and $M_{\text{DM}}-v_{\text{max}}$ relations from a sample of 120 late-type galaxies with rotational velocity measurements and dark matter halo masses estimated using the Di Cintio et al. (2014a) halo profile. Their halo profile model is derived from cosmological galaxy formation simulations, which account for baryonic processes affecting their host dark matter halos (Di Cintio et al. 2014a, 2014b; Artale et al. 2019), unlike cosmological dark matter-only simulations (Navarro et al. 1996).¹¹ Katz et al. (2018b) argue that tight relations between all of these choices for rotational velocity indicate that the kinematics of a late-type galaxy, at radii much smaller than its virial radius,¹² can be reliably used to estimate its halo mass.

Based on their sample of 120 late-type galaxies, they concluded that all of these different measures produce consistent results. We have elected to use v_{max} due to its ubiquity in published extragalactic HI source catalogs. Additionally, we assume that v_{max} is an accurate tracer of the circular velocity (v_{circ}) for spiral galaxies at large radii (i.e., $v_{\text{circ}} \equiv v_{\text{max}}$). We employ the $M_{\text{DM}}-v_{\text{max}}$ relation from Katz et al. (2018b), which is such that

$$\log\left(\frac{M_{\text{DM}}}{M_{\odot}}\right) = (2.439 \pm 0.196)\log\left(\frac{v_{\text{max}}}{138 \text{ km s}^{-1}}\right) + (11.552 \pm 0.108), \quad (5)$$

with total root mean square (rms) scatter $\Delta_{\text{rms}} = 0.244 \text{ dex}$ ¹³ in the $\log M_{\text{DM}}$ direction.¹⁴ We apply Equation (5) to the v_{max} values (Table 1, Column (6)) and list the derived dark matter halo masses in Table 1, Column (9).

3. Analysis and Discussion

3.1. The $v_{\text{max}}-\sigma_0$ Relation

The correlation between v_{rot} and σ_0 suggests a relationship between the dark matter halo and the stellar bulge of a galaxy, at least for galaxies with bulges. Ferrarese (2002) initially presented an empirical $v_{\text{rot}}-\sigma_0$ relation involving 38 spiral galaxies. Baes et al. (2003) followed up this work by adding a dozen spiral galaxies and found a consistent, tight correlation. Pizzella et al. (2005) then argued that the $v_{\text{rot}}-\sigma_0$ relation is different for

high- and low surface brightness galaxies, while Ho (2007, and later Sabra et al. 2015) showed from a large sample of 792 galaxies with diverse morphological types that the $v_{\text{rot}}-\sigma_0$ relation varies significantly for subsamples based on morphology. Courteau et al. (2007) subsequently showed that massive galaxies scattered about a $v_{\text{rot}} = \sqrt{2} \sigma_0$ relation (see Serra et al. 2016, who found $v_{\text{rot}} = 1.33 \sigma_0$ for early-type galaxies) and pure disks obeyed $v_{\text{rot}} \simeq 2 \sigma_0$, and they advocated that a trivariate relationship with total light concentration was needed to properly model the data.

Here, we produce a $v_{\text{max}}-\sigma_0$ relation for the 40 spiral galaxies with both v_{max} and σ_0 measurements (not including NGC 4395). Knowing σ_0 , this relation can be used to estimate v_{max} and indirectly predict M_{DM} (through Equation (5)); this is useful for galaxies with velocity dispersion measurements that lack reliable rotational velocity measurements (e.g., nearly face-on disk galaxies). The BCES *bisector* regression (Akritas & Bershady 1996; Nemmen et al. 2012)¹⁵ yields

$$\log\left(\frac{v_{\text{max}}}{\text{km s}^{-1}}\right) = (0.65 \pm 0.10)\log\left(\frac{\sigma_0}{141 \text{ km s}^{-1}}\right) + (2.34 \pm 0.01), \quad (6)$$

with $\Delta_{\text{rms}} = 0.08 \text{ dex}$ and intrinsic scatter¹⁶ $\epsilon = 0.07 \text{ dex}$, both in the $\log v_{\text{max}}$ direction (see Figure 1).

Except for NGC 4395, it is apparent from inspection of Figure 1 that five galaxies (Circinus, NGC 613, NGC 1300, NGC 4151, and NGC 5055) are mild outliers, noticeably outside the $\pm 1\sigma$ ($\pm 1 \Delta_{\text{rms}}$) scatter band. Of these five galaxies, two galaxies (NGC 1300 and NGC 5055) are $>2\sigma$ outliers. Davis et al. (2018) note that NGC 1300 is an outlier in the $M_{\text{BH}}-M_{*,\text{tot}}$ diagram for spiral galaxies, with either an overmassive black hole or a low total stellar mass, which is matched here by either a low v_{max} or a high σ_0 . Davis et al. (2017) pointed out that NGC 5055 is an outlier in the $M_{\text{BH}}-\sigma_0$ diagram for spiral galaxies, with either an overmassive black hole or a low central stellar velocity dispersion.

Our $(\sigma_0, v_{\text{max}})$ data set can be described by a Pearson correlation coefficient $r = 0.41$ and a p -value probability equal to 9.35×10^{-3} that the null hypothesis is true. The Spearman rank-order correlation coefficient $r_s = 0.40$, with $p_s = 1.07 \times 10^{-2}$ that the null hypothesis is true. However, the slope of the $v_{\text{max}}-\sigma_0$ relation is inconsistent with a value of 1 at the 3.5σ level. That is, v_{max}/σ_0 is not a constant ratio. We do, however, acknowledge that the $v_{\text{max}}-\sigma_0$ relation may be bent or curved, but we require more data with $\sigma_0 < 100 \text{ km s}^{-1}$ to see this. We find that the slope of our $v_{\text{max}}-\sigma_0$ relation is shallower than but consistent with the $v_{\text{rot}}-\sigma_0$ slope (0.84 ± 0.09) from Ferrarese (2002) for 38 spiral galaxies; the slope (0.74 ± 0.07) from Pizzella et al. (2005) for 40 high surface brightness disk galaxies, eight giant low surface brightness galaxies, and 24 elliptical galaxies; and the slope (0.90 ± 0.15) from Kormendy & Bender (2011) for 30 spiral galaxies, which are a subset of the Ferrarese (2002) sample; at the levels of 1.00σ , 0.53σ , and 1.00σ , respectively.

Our sample selection of only galaxies with dynamically estimated black hole masses does appear to have resulted in a selection bias, artificially truncating data such that we have a deficit of galaxies with $\sigma_0 \lesssim 100 \text{ km s}^{-1}$ (as seen in Figure 1). Lynden-Bell et al. (1988, their Figure 10) discuss this problem and present a solution by modifying the type of linear regression. By using a regression of $\log v_{\text{max}}$ on $\log \sigma_0$, i.e., the BCES($Y|X$)

¹¹ Katz et al. (2018b) also compared their results with halo masses derived from the Navarro et al. (1996) halo profile, but found poor results owing to “the cusp-core problem” for galaxies with slowly rising rotation curves (de Blok et al. 2001; de Blok & Bosma 2002; Gentile et al. 2004; Kuzio de Naray et al. 2006, 2008, 2009; Katz et al. 2017).

¹² Katz et al. (2018b) note that v_{flat} is generally measured at a radius farther out than the typical measurement radii of $v_{2.2}$, v_{eff} , or v_{max} , where the halo influence dominates the rotation curve. Even at the radius (r_{flat}) where v_{flat} is measured, they deduce that $\sim 93\%$ (on average) of a halo mass is external to r_{flat} .

¹³ Katz et al. (2018b) find an equivalent level of scatter (0.242 dex in $\log M_{\text{DM}}$) for the baryonic Tully–Fisher relation (Freeman 1999; Walker 1999; McGaugh et al. 2000) derived from the same sample of galaxies.

¹⁴ Because they used an unnormalized value of v_{max} by Katz et al. (2018b), the error on their intercept at $v_{\text{max}} = 0 \text{ km s}^{-1}$ is elevated through the inflated covariance between the slope and intercept (Tremaine et al. 2002). In Equation (5), we have estimated a normalization constant of 138 km s^{-1} with an associated intercept of 11.552 ± 0.108 from the upper right panel of Figure 2 in Katz et al. (2018b).

¹⁵ <https://github.com/rsnennen/BCES>

¹⁶ Calculated through Equation (1) from Graham & Driver (2007).

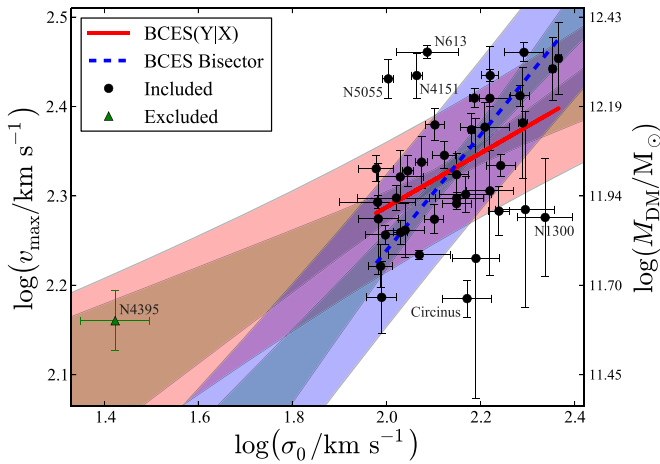


Figure 1. Maximum rotational velocity (and dark matter halo mass through Equation (5)) vs. central stellar velocity dispersion for 40 spiral galaxies (black filled dots), not including NGC 4395 (green triangle). Equation (6) is represented by the dashed blue line and Equation (7) is represented by the solid red line. The dark shaded region surrounding each line shows the $\pm 1\sigma$ uncertainty on the slope and the intercept from the regression, while the light shaded region delineates the $\pm 1\sigma$ scatter of the data about the regression line. Error bars denote the uncertainties on σ_0 and v_{\max} , the error bars associated with M_{DM} are not represented and are, in actuality, larger due to error propagation. The bulgeless galaxy NGC 4395 is additionally plotted, but not included in the regressions.

routine that minimizes the residuals in the Y -direction, we can generate a relation that is less strongly affected by this bias. Doing so, we find

$$\log\left(\frac{v_{\max}}{\text{km s}^{-1}}\right) = (0.30 \pm 0.11)\log\left(\frac{\sigma_0}{141 \text{ km s}^{-1}}\right) + (2.33 \pm 0.01), \quad (7)$$

with $\Delta_{\text{rms}} = 0.07$ dex and $\epsilon = 0.06$ dex, both in the $\log v_{\max}$ direction (see Figure 1).

Indeed, it is prudent to show concern for possible selection bias. Batcheldor (2010) pointed out that a false $M_{\text{BH}}-\sigma_0$ relation can be obtained from galaxies with randomly assigned black hole masses by imposing a spatial resolution cutoff to censor unresolvable spheres of influence. Thus, it is important to be cautious about unobserved data in samples of spiral galaxies with dynamical black hole mass estimates. However, it is also possible that the $v_{\max}-\sigma_0$ relation breaks down for small galaxies. For example, Courteau et al. (2007, see their Figure 1) show that the $v_{\max}-\sigma_0$ relation only holds for galaxies with $\sigma_0 \gtrsim 80 \text{ km s}^{-1}$ and $v_{\max} \gtrsim 200 \text{ km s}^{-1}$, and they attribute the breakdown for smaller galaxies to less certain rotational and dispersion estimates due to amplified gas turbulence, velocity anisotropy, and measurement errors.

3.1.1. Pseudobulges

Galaxies that allegedly contain pseudobulges¹⁷ constitute the bulk of our sample (i.e., 36 out of 42; Davis et al. 2017). For

¹⁷ See Fisher & Drory (2016) for a review, summarizing the observed properties of pseudobulges and classical bulges, and see Graham (2015) for concerns with identifying pseudobulges, splitting what may be a bulge continuum, and galaxies hosting both types of bulge (see Izquierdo-Villalba et al. 2019, for semianalytical models of galaxy formation yielding composite bulges). Equally concerning, Costantin et al. (2018) assess that bulge classification is difficult with any observational diagnostic other than their intrinsic three-dimensional shape: classical bulges appear as thick oblate spheroids, with pseudobulges distinguishable by their relative disk-like flattening.

local ($z \sim 0$) galaxies, the central stellar velocity dispersion is primarily a measurement of the kinematics of the bulge; however, for galaxies with only pseudobulges or small bulges, the kinematics of the bar and disk will contribute in a higher proportion than the weak contribution in galaxies with large classical bulges (Courteau et al. 2007).¹⁸ Hartmann et al. (2014) show that the central σ_0 is not only $\sigma_0(\text{bulge})$ but rather $\sigma_0(\text{bulge} + \text{disk})$ due to contamination by the disk, which increases with disk inclination. When a classical bulge does not dominate, it is important to take into account the disk, the effect of gas (whereas the gas is negligible in massive galaxies and ellipticals), the bar orientation,¹⁹ the spectral line used for the measurement,²⁰ the rotation,²¹ and the inclination. These complications are beyond the scope of this project; however, we might suspect a dependency on inclination for our sample, especially for the galaxies with the lowest observed σ_0 values, where disk star contamination (if present) will be fractionally more noteworthy. An additional investigation of the bar strength is beyond the desired scope of this work; however, a significant follow-up study might garner further insight. For example, NGC 613 and NGC 1300 (both classical barred galaxies) are prominent outliers in Figure 1, suggesting that their bars might have significantly altered the kinematics of these galaxies.

Graham et al. (2011) demonstrate that the scatter in the $M_{\text{BH}}-\sigma_0$ diagram can be mitigated by fitting an offset relation for barred galaxies. For pseudobulges built from bars, the “bulge” is very flattened, and the velocity dispersion is anisotropic, much larger in the horizontal than in the vertical direction. Bellovary et al. (2014) specifically treat this anisotropic issue, and show that increased inclination not only produces an elevated scatter at the low-mass end of the $M_{\text{BH}}-\sigma_0$ relation, but also introduces a bias, to increase globally both the average and the median value above the true σ_0 , which tends to show an offset $M_{\text{BH}}-\sigma_0$ relation for disky galaxies. This bias applies not just to barred galaxies but to all spiral galaxies because all spiral galaxies will likely possess a bar at some point in their life. Sheth et al. (2008) describe the development of a bar as an indicator of maturity, although bars may be recurrent and therefore not a sign of either maturity or immaturity.

In consideration of the effects of inclination, we have investigated σ_0 versus $\sin(i)$ and found no correlation. We do, however, note that some galaxies have uncharacteristically low σ_0 values. For instance, NGC 253 (the Sculptor galaxy) has $\sigma_0 = (96 \pm 18) \text{ km s}^{-1}$, but it is a bulgy, massive, and inclined ($i = 75^\circ.3$) galaxy. Perhaps some explanation for this galaxy can be obtained by considering that NGC 253 is a prototypical starburst galaxy (Watson et al. 1996; Kornei & McCrady 2009; Leroy et al. 2018;

¹⁸ Similarly, the use of σ_e (the velocity dispersion within the effective half-light radius of a galaxy) is not desirable because it is heavily biased by any bar or disk in the galaxy.

¹⁹ Bars, when viewed from an end-on orientation, may exhibit a small secondary biasing effect. Sight-lines down the major axis of a bar should elevate the observed σ_0 , and thus more edge-on disks would have higher σ_0 values if the bar were additionally positioned in the right way within the disk plane for this sight-line to occur.

²⁰ Harris et al. (2012) point out that the spectral line used for the measurement of σ_0 can bias the result by as much as 8%.

²¹ Spectroscopic measurements of velocity dispersion through a fixed aperture do not yield reliable estimates for the true σ_0 of a galaxy due to contamination from galactic rotation (Taylor et al. 2010; Bezanson et al. 2011; van Uitert et al. 2013; Hasan & Crocker 2019). Kang et al. (2013) address the problem of rotation contaminating the σ_0 measurement and try to remove the rotation and isolate the true σ_0 with small apertures. They report consistent σ_0 values from the optical and near-infrared absorption lines, but find that a rotation component can cause σ_0 to vary by up to $\sim 20\%$ in a single-aperture spectrum.

Mangum et al. 2019; Martin et al. 2019; Takano et al. 2019). As a result, σ_0 may depend on the age of the stars: when there is gas, young stars can form from the gas, strongly weight the optical spectrum, and “cool” the stellar component.²² This process in the disk can contribute to the measurement of σ_0 , leading to a small σ_0 -drop at the center of a galaxy and could explain why σ_0 is low for NGC 253 and other star-forming galaxies. Indeed, other prominent starburst galaxies display this behavior. The v_{\max}/σ_0 ratios of NGC 253 and three other prominent star-forming galaxies, IC 342, NGC 2146, and NGC 6946 (see Gorski et al. 2018, and references therein), are all elevated with $v_{\max}/\sigma_0 = 2.04 \pm 0.38$, 3.11 ± 0.49 , 2.33 ± 0.16 , and 5.66 ± 0.98 (all from HyperLeda), respectively. Moreover, the bar in NGC 253 is not end-on but inclined (if not completely side-on), reducing its effect on σ_0 .

The widespread presence of low- to medium-luminosity active galactic nuclei (AGNs) in spiral galaxies (e.g., Beifiori et al. 2009; Jiang et al. 2011; Xiao et al. 2011) indicates that the efficient growth of SMBHs through the accretion of gas is prevalent. It is evident that secular processes in disk galaxies play a key role in the development of SMBHs (Cisternas et al. 2011; Schawinski et al. 2011, 2012; Araya Salvo et al. 2012; Kocevski et al. 2012; Simmons et al. 2012; Treister et al. 2012; Debattista et al. 2013; Zubovas & King 2019). Nuclear bars have been theorized to drive gas inflows into the center, feeding black holes (e.g., Shlosman et al. 1989, 1990; Hopkins & Quataert 2010). Du et al. (2017; see also Valluri et al. 2016) considered the effect of an SMBH on a nuclear bar, showing that nuclear bars are destroyed at lower SMBH masses than the large-scale bars in their simulations. Specifically, they found that embedded bars are quickly dissolved when $M_{\text{BH}} \gtrsim 0.2\% M_{*,\text{tot}}$, halting the inner-bar-driven gas-feeding mechanism. For comparison, we find that for the subsample of 35 pseudobulge spiral galaxies in Davis et al. (2018), the median ratio is is approximately an order of magnitude lower, $M_{\text{BH}} = (0.016\% \pm 0.011\%)M_{*,\text{tot}}$.

The central velocity dispersion is enhanced by the presence of a bar, ultimately leading to slightly higher values of σ_0 in barred galaxies than in unbarred galaxies. Hartmann et al. (2014) conducted simulations, showing that bar growth heats the disk, forms the bulge, and concentrates the mass,²³ therefore the mass evolution increases the central velocity dispersion,²⁴ which causes barred galaxies to move to higher

velocity dispersions in the $M_{\text{BH}}-\sigma_0$ diagram. However, their simulations did not include gas (see Seo et al. 2019), which meant that gas was not present to possibly form new stars (cooling the stellar component and decreasing σ_0) or fuel SMBHs in their galaxies (increase M_{BH}). From complementary simulations, Brown et al. (2013) found that the growth of an SMBH also affects the nuclear stellar kinematics of a galaxy, increasing σ_0 .²⁵

3.1.2. The $M_{\text{DM}}-\sigma_0$ Relation

As mentioned in Section 1, some theoretical models suggest that dark matter halos should be related to the mass of their SMBHs. Additionally, lambda cold dark matter (Λ CDM) disk–bulge–halo models indicate that disks and bulges are formed from the cooling of baryons inside dark matter halos, implying that the disk and bulge of a galaxy should also be partially determined by the properties of its dark matter halo (e.g., Haehnelt et al. 1998; van den Bosch 2000; Zhang & Wyse 2000). As a consequence of this bulge–halo connection and the known $M_{\text{BH}}-\sigma_0$ relation, there should be an $M_{\text{DM}}-\sigma_0$ correlation. Combining our $v_{\max}-\sigma_0$ relation (Equation (6)) with Equation (5) yields

$$\log\left(\frac{M_{\text{DM}}}{M_{\odot}}\right) = (1.58 \pm 0.29)\log\left(\frac{\sigma_0}{141 \text{ km s}^{-1}}\right) + (12.03 \pm 0.12). \quad (8)$$

Additional uncertainty is introduced through the propagation of errors²⁶ when Equations (6) and (5) are combined, however, Equation (8) provides a useful method of quickly estimating M_{DM} in spiral galaxies with bulges when only σ_0 measurements are available.

Zahid et al. (2016) examine the $\sigma_0-M_{*,\text{tot}}$ relation for massive ($M_{*,\text{tot}} \gtrsim 10^{10.3} M_{\odot}$) quiescent galaxies at $z < 0.7$. They find that $\sigma_0 \propto M_{*,\text{tot}}^{0.3}$, which is the same as the scaling relation between the dark matter halo velocity dispersion and halo mass (i.e., $\sigma_{\text{DM}} \propto M_{\text{DM}}^{0.3}$) obtained by N -body simulations (Evrard et al. 2008; Posti et al. 2014). We can compare our result by rearranging Equation (8) to show that $\sigma_0 \propto M_{\text{DM}}^{0.63 \pm 0.11}$ for late-type galaxies has twice the slope derived by Zahid et al. (2016) for early-type galaxies.

To the best of our knowledge, this is the first time that the relationship between the mass of the dark matter halo and the central stellar velocity dispersion has been derived or presented for spiral galaxies, although we caution against its extrapolation to late-type (\gtrsim Sc) spiral galaxies with $\sigma_0 \lesssim 100 \text{ km s}^{-1}$ that potentially are overinfluenced by the disk kinematics. Alternatively, combining Equation (7) with Equation (5) yields

$$\log\left(\frac{M_{\text{DM}}}{M_{\odot}}\right) = (0.74 \pm 0.26)\log\left(\frac{\sigma_0}{141 \text{ km s}^{-1}}\right) + (12.03 \pm 0.12). \quad (9)$$

²² This is contrary to a collision-less simulation, where the stellar component only heats up.

²³ The bar strength is not necessarily a clear indicator of mass concentration, as a galaxy could have already passed its maturity, concentrated its mass, and its once strong bar could now appear weakened or have disappeared.

²⁴ The simulations of Hartmann et al. (2014) show that the formation of a bar yields an elevated σ_0 even when viewing the disk face-on. This suggests a connection with out-of-plane buckling that leads to peanut-shell-shaped structures (Burbidge & Burbidge 1959; de Vaucouleurs 1974; Illingworth 1983; Jarvis 1986; Combes et al. 1990; Bureau & Freeman 1999; Lütticke et al. 2000a, 2000b; Patsis et al. 2002; Buta et al. 2007; Athanassoula 2016; Ciambur & Graham 2016) that are more readily visible in edge-on spiral galaxies, but are also recognizable in more face-on systems (Laurikainen et al. 2011, 2013, 2014, 2015, 2018; Erwin & Debattista 2013; Athanassoula et al. 2015; Buta et al. 2015; Laurikainen & Salo 2016; Herrera-Endoqui et al. 2017; Laurikainen & Salo 2017; Salo & Laurikainen 2017a, 2017b; Saha et al. 2018). The bar or peanut shell shape may also increase the vertical dispersion of the disk, in addition to the bar, but this is a small effect considering the great streaming in the disk. Therefore, if Hartmann et al. (2014) see an effect for $i = 0^\circ$, it is more likely due to the concentration of the mass in the center and the global heating than due to the peanut shell shape. Moreover, when gas is present, there is a diminished box or peanut-shell-shape effect; the presence of a large gas fraction tends to weaken or destroy the peanut shell shape.

²⁵ Hartmann et al. (2014) remark that the increase in σ_0 due to SMBH growth within a bar, seen by Brown et al. (2013), is only a small effect ($\sim 7\%$) compared to that resulting from the formation and evolution of a bar.

²⁶ Error propagation calculations were performed with the PYTHON package UNCERTAINTIES (<http://pythonhosted.org/uncertainties/>).

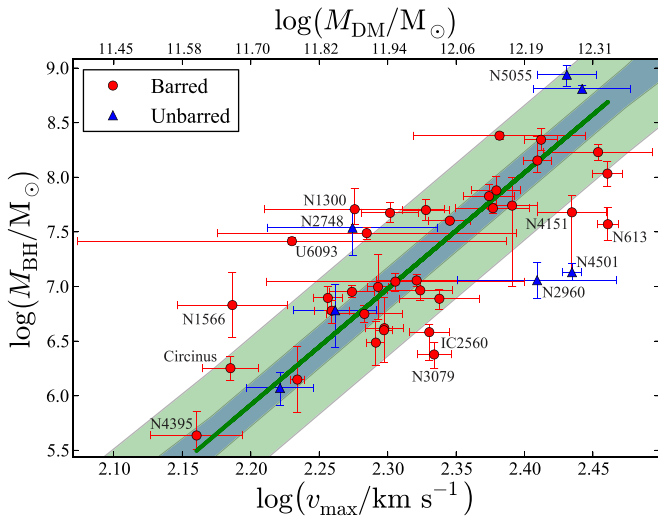


Figure 2. Black hole mass vs. maximum rotational velocity (and dark matter halo mass according to Equation (5)) for 42 galaxies. Equation (10) is depicted by the green line. Galaxies with barred morphologies are represented by red dots, and those without bars are represented by blue triangles.

3.2. The $M_{\text{BH}}-v_{\text{max}}$ Relation

Here, we derive the $M_{\text{BH}}-v_{\text{max}}$ scaling relation for the largest sample of spiral galaxies with directly measured black hole masses to date. Our $(v_{\text{max}}, M_{\text{BH}})$ data set, consisting of 42 galaxies, can be described by $r = 0.74$, $p = 2.24 \times 10^{-8}$, $r_s = 0.72$, and $p_s = 6.70 \times 10^{-8}$. The BCES bisector regression yields the relation

$$\log\left(\frac{M_{\text{BH}}}{M_{\odot}}\right) = (10.62 \pm 1.37)\log\left(\frac{v_{\text{max}}}{210 \text{ km s}^{-1}}\right) + (7.22 \pm 0.09), \quad (10)$$

with $\Delta_{\text{rms}} = 0.58$ dex and $\epsilon = 0.45$ dex, both in the $\log M_{\text{BH}}$ direction (see Figure 2). These levels of scatter place the $M_{\text{BH}}-v_{\text{max}}$ relation on par with the scatter ($\Delta_{\text{rms}} = 0.63$ dex and $\epsilon = 0.58$ dex) about the $M_{\text{BH}}-\sigma_0$ relation for spiral galaxies (Davis et al. 2017).

The slope for the $M_{\text{BH}}-v_{\text{max}}$ relation is significantly steeper than the slopes presented in previous works. However, the steep slope is in good agreement with the prediction from Equation (3), consistent at the level of 0.46σ , which both confirms that our $M_{\text{BH}}-v_{\text{max}}$ relation is in agreement with the Tully–Fisher relation and that the $M_{\text{BH}}-M_{*,\text{tot}}$ relation must have the steep slope of ≈ 3 reported by Davis et al. (2018).²⁷

We do not find barred galaxies to be offset in our $M_{\text{BH}}-v_{\text{max}}$ relation (see Figure 2); the bulk of our galaxies have barred morphologies (35 out of 42). Courteau et al. (2003) found that barred galaxies are not offset in the Tully–Fisher relation, reinforcing our finding that v_{max} appears to predict black hole masses equally well for barred and nonbarred galaxies.²⁸ That

²⁷ For reference, the $M_{\text{BH}}-(\text{stellar bulge mass})$ relation for spiral galaxies has a slope of $2.44^{+0.35}_{-0.31}$ (Davis et al. 2019).

²⁸ In a highly influential work, Ostriker & Peebles (1973) concluded from their simulations of galaxies that massive halos would act to stabilize disks and suppress bar instabilities; thus, bars would preferentially form in galaxies with low-concentration halos. However, we now know that this is wrong. Bosma (1996) remark on the stabilizing influence of a bulge, and Sellwood & Evans (2001) find that high central rates of shear can stabilize a disk regardless of the dark matter halo density. In fact, the halo does not stabilize the disk, and even in some cases destabilizes it by increasing the bar instability (Athassoula 2002).

is, a single $M_{*,\text{tot}}-v_{\text{max}}$ Tully–Fisher relation for spiral galaxies combined with a single $M_{\text{BH}}-M_{*,\text{tot}}$ relation for spiral galaxies yields a single $M_{\text{BH}}-v_{\text{max}}$ relation for spiral galaxies.

Based on the behavior of four spiral galaxies, Ferrarese (2002) postulated that halos with $M_{\text{DM}} \lesssim 5 \times 10^{11} M_{\odot}$, i.e., $\log(M_{\text{DM}}/M_{\odot}) \lesssim 11.70$, are progressively less efficient or perhaps incapable of forming SMBHs.²⁹ As can be seen in Figure 2, three of our galaxies (Circinus, NGC 1566, and NGC 4395, two of which were outliers in Figure 1) have $\log(M_{\text{DM}}/M_{\odot}) < 11.70$ (i.e., $v_{\text{max}} < 159 \text{ km s}^{-1}$ from Equation (5)). Our results show that $5 \times 10^{11} M_{\odot}$ is not a hard-and-fast threshold; however, given that our uncertainties on $\log M_{\text{DM}}$ are greater than ± 0.1 dex (see Table 1, Column (9)), our smallest dark matter halos are only marginally below this limit. For example, based on $v_{\text{max}} = 98 \pm 7 \text{ km s}^{-1}$, we predict that NGC 1566 has a quite low $\log(M_{\text{DM}}/M_{\odot}) = 11.67 \pm 0.15$. However, because NGC 1566 is a Type I Seyfert galaxy (Alloin et al. 1985; Oknyansky et al. 2019), it is hard to imagine it not possessing an SMBH.

If we track the location of the six outliers from Figures 1 to 2, we find that the locations of NGC 613, NGC 1300, and NGC 4151 suggest that their maximum rotational velocities are anomalous, rather than their central stellar velocity dispersions or black hole masses. Circinus, NGC 4395, and NGC 5055 are not outliers in Figure 2, indicating that they might have abnormal central stellar velocity dispersions, rather than deviant maximum rotational velocities or black hole masses. NGC 4501 is the most significant outlier in Figure 2. It was not an outlier in Figure 1, implying that the black hole might be undermassive, although it was not an outlier in any of our past black hole mass scaling relations with σ_0 , ϕ , stellar bulge mass, or stellar galaxy mass.

The $M_{\text{BH}}-v_{\text{rot}}$ relation (and/or the $M_{\text{BH}}-M_{\text{DM}}$ relation, see Section 3.2.1) have been studied for nearly two decades (Ferrarese 2002; Baes et al. 2003; Zasov et al. 2005; Sabra et al. 2008; Kormendy & Bender 2011; Volonteri et al. 2011; Beifiori et al. 2012; Sun et al. 2013; Sabra et al. 2015). These studies have been conducted on varied galaxy samples, including all manner of morphological types, black hole mass estimates, measures of rotational velocities, and linear regression routines. The published results for the $M_{\text{BH}}-v_{\text{rot}}$ relations have been quite diverse, ranging from a null result (Kormendy & Bender 2011) to a shallow slope of $M_{\text{BH}} \propto v_{\text{rot}}^{2.28 \pm 0.67}$ (Sabra et al. 2015) and up to $M_{\text{BH}} \propto v_{\text{rot}}^{7.60 \pm 0.40}$ (Volonteri et al. 2011). None of these results are steep enough to give consistency between the $M_{\text{BH}}-M_{*,\text{tot}}$ (Equation (2)) and Tully–Fisher (Equation (1)) relations for spiral galaxies.

Some of the explanation for why all previous studies seem to have underestimated the slope of the $M_{\text{BH}}-v_{\text{rot}}$ relation lies in an almost ubiquitous adoption of a nearly linear $M_{\text{BH}}-M_{*,\text{tot}}$ relation. If this were true, then our earlier prediction (Equation (3)) would become $M_{\text{BH}} \propto M_{*,\text{tot}} \propto v_{\text{rot}}^{4.0 \pm 0.1}$, which lies in the middle of the findings to date. Such a slope might conceivably make some sense for a population of massive elliptical galaxies that have formed from the result of many mergers, but even then, Sahu et al. (2019) find $M_{\text{BH}} \propto M_{*,\text{tot}}^{1.65 \pm 0.11}$ for early-type galaxies as a whole, and, $M_{\text{BH}} \propto M_{*,\text{tot}}^{1.47 \pm 0.18}$ for core-Sérsic early-type galaxies. A linear $M_{\text{BH}}-M_{*,\text{tot}}$ relation is therefore closer to reality for early-type

²⁹ Alternatively, van Wassenhove et al. (2010) find that a few percent of their simulated galaxies with massive black holes encounter stripping during their evolution, which leaves them “naked,” having lost most of their surrounding dark matter halos.

galaxies, stellar orbits are more random, and both kinematical measures, σ_0 and v_{rot} , are well correlated (Zasov et al. 2005; Courteau et al. 2007; Ho 2007) and roughly consistent with $v_{\text{circ}} = \sqrt{2}\sigma_0$ for the singular isothermal sphere profile, such that a collision-less system of stars is identical to an isothermal self-gravitating sphere of gas (Binney & Tremaine 2011). However, none of this applies to low-mass spiral galaxies, which have been historically underrepresented in black hole mass scaling relations.

One additional factor depressing the slopes of some past studies of the $M_{\text{BH}}-M_{*,\text{tot}}$ and $M_{\text{BH}}-v_{\text{rot}}$ relations has been the inclusion of early-type galaxies in their samples. Sahu et al. (2019) find that early-type galaxies follow a different $M_{\text{BH}}-M_{*,\text{tot}}$ relation than late-type galaxies, with early-type galaxies with disks (ES/S0) exhibiting $M_{\text{BH}} \propto M_{*,\text{tot}}^{1.94 \pm 0.21}$. Because most early-type galaxies contain disks (e.g., Emsellem et al. 2011; Krajnović et al. 2011), and lenticular galaxies also follow the Tully–Fisher relation (Williams et al. 2009), for lenticular galaxies, Equation (3) would become $M_{\text{BH}} \propto v_{\text{rot}}^{7.8 \pm 0.9}$, a result that is most similar to the results of Sabra et al. (2008)³⁰ and Volonteri et al. (2011), consistent at the level of 0.62σ and 0.15σ , respectively.

3.2.1. The $M_{\text{BH}}-M_{\text{DM}}$ Relation

Observations find AGN in galaxies with little or no bulge (Satyapal et al. 2007, 2008) and thus hint at a possible underlying correlation between dark matter mass and black hole mass, rather than between bulge mass and black hole mass (Treuthardt et al. 2012). Such observations elevate the possibility of an $M_{\text{BH}}-M_{\text{DM}}$ relation (with M_{DM} coming from v_{max} through Equation (5)) in bulgy and bulgeless spiral galaxies, which might indicate that it is the cornerstone of black hole mass scaling relations. However, AGN feedback scenarios (e.g., Debuhr et al. 2010) suggest that the best correlation should be with the total baryonic mass rather than with the dark matter halo mass (if it is not the bulge mass) because the dark matter halo is mostly outside the baryons, and might not have much effect on the gas inflow to fuel the central SMBH. This means that the $M_{\text{BH}}-M_{\text{DM}}$ relation would be an indirect result of the $M_{\text{BH}}-(\text{total baryonic mass})$ relation.

Theoretical models suggest that the $M_{\text{BH}}-M_{\text{DM}}$ relation should be nonlinear. Haehnelt et al. (1998) demonstrated that the mass function of dark matter haloes could be matched to the $z = 3$ luminosity function for quasars with lifetimes in the range of 10^6-10^8 yr. Their models show a strong correlation between the lifetime of quasars and the slope of the $M_{\text{BH}}-M_{\text{DM}}$ relation, supporting longer quasar lifetimes as the slope of the $M_{\text{BH}}-M_{\text{DM}}$ relation becomes progressively steeper; a linear relationship would require quasar lifetimes shorter than 10^6 yr. Silk & Rees (1998) and Haehnelt et al. (1998) posited that $M_{\text{BH}} \propto M_{\text{DM}}^{5/3}$ (here, the typical quasar lifetime is a few times 10^7 yr) for an isothermal sphere of cold dark matter, where a proportionality exists between the energy injected by a black hole and the gravitational binding energy ($\propto GM^2/R$) of the halo.

Alternatively, Di Matteo et al. (2003) suggested that $M_{\text{BH}} \propto M_{\text{DM}}^{4/3}$, based on their Λ CDM cosmological hydrodynamic simulations. Booth & Schaye (2010) concluded that M_{BH} is

³⁰ Sabra et al. (2008) obtained $M_{\text{BH}} \propto v_{\text{rot}}^{6.75 \pm 0.80}$ from a sample consisting of approximately early-type galaxies. Seven years later, Sabra et al. (2015) found conflicting results between the relation fit from their data ($M_{\text{BH}} \propto v_{\text{rot}}^{2.28 \pm 0.67}$) and their prediction ($M_{\text{BH}} \propto v_{\text{rot}}^{5.15}$) from the observational study of galaxies by Bandara et al. (2009).

determined primarily by M_{DM} and found agreement with the isothermal prediction of Silk & Rees (1998) and Haehnelt et al. (1998), with $M_{\text{BH}} \propto M_{\text{DM}}^{1.55 \pm 0.05}$, which is itself in exact agreement with the observational study of Bandara et al. (2009), who find $M_{\text{BH}} \propto M_{\text{DM}}^{1.55 \pm 0.31}$ ³¹. However, these results should not be considered applicable to spiral galaxies as these studies focused on massive galaxies, e.g., the sample of Bandara et al. (2009) consisted of galaxies with $M_{\text{BH}} \gtrsim 10^8 M_{\odot}$ and $M_{\text{DM}} \gtrsim 10^{13} M_{\odot}$. Other published slopes for this relation, from galaxies with M_{BH} estimates, include $M_{\text{BH}} \propto M_{\text{DM}}^{1.65-1.82}$ (Ferrarese 2002) for 38 spiral galaxies and $M_{\text{BH}} \propto M_{\text{DM}}^{1.27}$ (Baes et al. 2003) for 50 spiral galaxies.

Recently, Mutlu-Pakdil et al. (2018) found $M_{\text{BH}} \propto M_{\text{DM}}^{1.55 \pm 0.02}$ from a new set of simulations (Vogelsberger et al. 2014), which is in precise agreement with the above findings (Bandara et al. 2009; Booth & Schaye 2010). Their work is different from previous studies because it focused on extending the relation to lower-mass spiral galaxies. However, their precise agreement with past studies of high-mass galaxies and an isothermal model indicate that their simulations remain tied or tuned to the old black hole mass scaling relations that assume that black holes and their host galaxies follow a nearly linear $M_{\text{BH}}-M_{*,\text{tot}}$ relation. Specifically, Mutlu-Pakdil et al. (2018) perceive that $M_{\text{BH}} \propto M_{*,\text{tot}}^{1.53 \pm 0.02}$, with a slope half as steep as our result for late-type galaxies (Equation (2)), but consistent with the relation $M_{\text{BH}} \propto M_{*,\text{tot}}^{1.65 \pm 0.11}$ for early-type galaxies from Sahu et al. (2019).³² Combining the results of Mutlu-Pakdil et al. (2018), $M_{\text{BH}} \propto M_{*,\text{tot}}^{1.53 \pm 0.02} \propto M_{\text{DM}}^{1.55 \pm 0.02}$, would suggest that the $M_{*,\text{tot}}-M_{\text{DM}}$ relation is almost exactly linear.

Evolutionary studies show how the $M_{*,\text{tot}}-M_{\text{DM}}$ relation changes with time (Hansen et al. 2009; Behroozi et al. 2010, 2013, 2019; Moster et al. 2010, 2013, 2018; Leauthaud et al. 2012; Yang et al. 2012; Reddick et al. 2013; Wang et al. 2013; Birrer et al. 2014; Lu et al. 2015; Rodríguez-Puebla et al. 2017; Kravtsov et al. 2018; Mowla et al. 2019). Tiley et al. (2019) performed an analysis of the Tully–Fisher relation at $z \approx 0$ and $z \approx 1$ by carefully comparing local and distant samples of late-type galaxies and degrading the quality of the local sample to match that of the distant sample. They concluded that no significant difference is apparent between the two epochs, suggesting an intimate link between stellar mass and dark matter (as traced by v_{max}) in late-type galaxies over at least an ≈ 8 Gyr period.

The $M_{*,\text{tot}}-M_{\text{DM}}$ relation is traditionally fit with a double power law, exhibiting a steep low-mass slope and a shallow high-mass slope (Yang et al. 2012; Moster et al. 2013).³³ For the low-mass portion of the double power-law $M_{*,\text{tot}}-M_{\text{DM}}$ relation, Katz et al. (2018a) speculate that late-type galaxies should follow a theoretical $M_{*,\text{tot}} \propto M_{\text{DM}}^{5/3}$ relation, powered by supernovae feedback and its role in regulating galaxy formation. Furthermore, Katz et al. (2018a) follow this theoretical prediction up with an observational determination of $M_{*,\text{tot}} \propto M_{\text{DM}}^{1.51 \pm 0.13}$ from their sample of late-type galaxies

³¹ See also the observational study by Bogdán & Goulding (2015), who find $M_{\text{BH}} \propto M_{\text{DM}}^{1.6 \pm 0.4}$ from a sample of 3130 elliptical galaxies.

³² From inspection of Figures 7 and 8 from Mutlu-Pakdil et al. (2018), we point out an apparent bend in the respective scaling relations with black hole mass. There is a noticeable dichotomy between low- and high-mass black holes, such that it warrants a steeper slope for spiral galaxies hosting low-mass black holes and a shallow slope for early-type galaxies hosting high-mass black holes, rather than their single regression fit to the combined sample.

³³ However, Behroozi et al. (2013) note that a pure double power law is not perfect and results in a $M_{\text{BH}}-M_{\text{DM}}$ relation that is off by as much as 0.1 dex.

from the SPARC sample with Di Cintio et al. (2014a) dark matter halo profiles. Combining this result with Equation (2) necessarily implies that

$$M_{\text{BH}} \propto M_{\text{DM}}^{4.61 \pm 0.89}. \quad (11)$$

Combining our spiral galaxy $M_{\text{BH}}-v_{\text{max}}$ relation (Equation (10)) with Equation (5) yields

$$\log\left(\frac{M_{\text{BH}}}{M_{\odot}}\right) = (4.35 \pm 0.66)\log\left(\frac{M_{\text{DM}}}{10^{12} M_{\odot}}\right) + (7.22 \pm 0.12), \quad (12)$$

which is consistent with the slope from Equation (11) at the level of 0.17σ . This slope for spiral galaxies is notably steeper than reported in past studies (e.g., Haehnelt et al. 1998; Silk & Rees 1998; Ferrarese 2002; Baes et al. 2003; Bandara et al. 2009; Booth & Schaye 2010; Bogdán & Goulding 2015; Mutlu-Pakdil et al. 2018).

3.3. The $v_{\text{max}}-\phi$ Relation

The maximum rotational velocity does not only correlate with M_{BH} (Figure 2), but also with, among other things, the spiral-arm pitch angle, ϕ (for an introduction, see Davis et al. 2017).³⁴ Kennicutt (1981) observed a correlation between the maximum rotational velocity and the spiral-arm pitch angle, which was later reanalyzed and quantified by Savchenko & Reshetnikov (2011). Kennicutt (1981) described the anticorrelation as being “fairly strong,”³⁵ and claimed that it supports the density-wave theory expectations for spiral-arm geometry (Roberts et al. 1975).³⁶

Our $(\tan|\phi|, \log v_{\text{max}})$ data set of 42 galaxies can be described by $r = -0.62$, $p = 1.31 \times 10^{-5}$, $r_s = -0.58$, and $p_s = 5.73 \times 10^{-5}$. The BCES *bisector* regression yields

$$\log\left(\frac{v_{\text{max}}}{\text{km s}^{-1}}\right) = (-0.85 \pm 0.14)[\tan|\phi| - \tan 13^{\circ}35'] + (2.33 \pm 0.01), \quad (13)$$

with $\Delta_{\text{rms}} = 0.07$ dex and $\epsilon = 0.05$ dex, both in the $\log v_{\text{max}}$ direction (see Figure 3).

The outliers in Figure 3 match the behavior in the $M_{\text{BH}}-v_{\text{max}}$ diagram (Figure 2). This reflects the tight $M_{\text{BH}}-\phi$ relation (Seigar et al. 2008; Berrier et al. 2013; Davis et al. 2017). However, NGC 2748 was an outlier in the $M_{\text{BH}}-\phi$ diagram (Davis et al. 2017), suggesting that its continued deviance in the $v_{\text{max}}-\phi$ diagram (Figure 3) is more due to its irregular spiral arms than to its maximum rotational velocity measurement because it was not an outlier in the $v_{\text{max}}-\sigma_0$ diagram (Figure 1).

Kennicutt (1981) qualitatively investigated the $v_{\text{max}}-\phi$ relation using a sample of 113 spiral galaxies, but he did not perform a linear regression. Savchenko & Reshetnikov (2011) culled the sample from Kennicutt (1981) down to a subsample

³⁴ Logarithmic spirals have been adopted as the natural metric for the form of spiral arms in disk galaxies since the pioneering works of von der Pahlen (1911), Groot (1925), Reynolds (1925), Lindblad (1927, 1938, 1941), and Danver (1942).

³⁵ Kendall et al. (2011, 2015) present a study of ϕ versus v_{flat} from near-infrared *Spitzer Space Telescope* imaging and “find no evidence for the strong anticorrelation” that was found in the optical by Kennicutt & Hodge (1982).

³⁶ See the recent reviews on spiral structure in disk galaxies (Dobbs & Baba 2014) and spiral density wave theory (Shu 2016) for additional information and historical context.

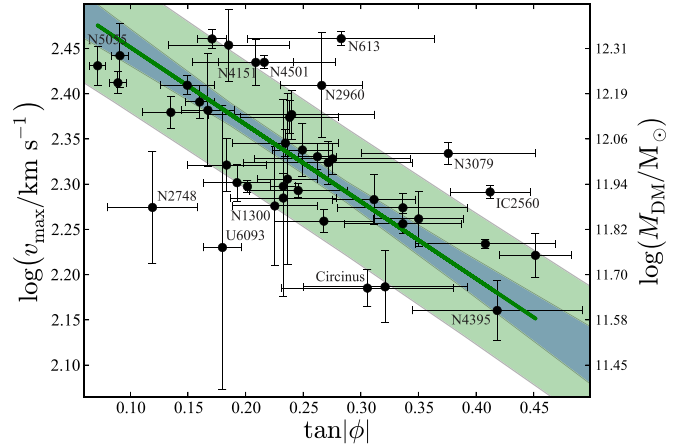


Figure 3. Maximum rotational velocity (and dark matter halo mass according to Equation (5)) vs. the tangent function of the spiral-arm pitch angle absolute value for our sample of 42 spiral galaxies. Equation (13) is represented by the green line.

of 46 galaxies and performed a linear (not a power-law) regression, yielding

$$|\phi| = (-0.049 \pm 0.008)\left(\frac{v_{\text{max}}}{\text{km s}^{-1}}\right) + (22^{\circ}85 \pm 1^{\circ}76). \quad (14)$$

When we perform a similar regression on our $(v_{\text{max}}, |\phi|)$ data set of 42 spiral galaxies, we find that the BCES *bisector* regression yields

$$|\phi| = (-0.127 \pm 0.019)\left(\frac{v_{\text{max}} - 210 \text{ km s}^{-1}}{\text{km s}^{-1}}\right) + (14^{\circ}43 \pm 0^{\circ}66), \quad (15)$$

with $\Delta_{\text{rms}} = 4^{\circ}36$ and $\epsilon = 3^{\circ}48$ in pitch angle. Our slope of -0.127 ± 0.019 is more than 2.5 times as steep as their slope. However, we argue that the slope of Savchenko & Reshetnikov (2011) in Equation (14) is too shallow because their zero-point predicts that $v_{\text{max}} = 0$ at $|\phi| = 22^{\circ}85 \pm 1^{\circ}76$. In contrast, our zero-point would predict that $v_{\text{max}} = 0$ at $|\phi| = 41^{\circ}11 \pm 3^{\circ}92$, which is on par with some of the highest measured pitch angle measurements in the literature. Nevertheless, such a formulation of the $v_{\text{max}}-\phi$ relation is inherently limited, given that v_{max} equals zero at high ϕ , which should not be the case. Only a rotating disk can have a spiral pattern with a measurable pitch angle. We prefer our formulation of the $v_{\text{max}}-\phi$ relation in Equation (13), where v_{max} never equals zero. Because ϕ is defined such that $0^{\circ} \leq |\phi| \leq 90^{\circ}$, the best-fit values from Equation (13) yield $340 \geq v_{\text{max}}/\text{km s}^{-1} > 0$, respectively.

Savchenko & Reshetnikov (2011) used the $z \sim 0$ correlation to predict v_{max} for a distant sample of galaxies in the *Hubble Deep Fields* (Ferguson et al. 2000; Beckwith et al. 2006) and ultimately concluded that the distant galaxies follow the local Tully–Fisher relation if they follow the local $v_{\text{max}}-\phi$ relation that they derived (for which we just doubled the slope). Given that Tiley et al. (2019) observe no significant difference between the zero-points³⁷ of the Tully–Fisher relation at $z \approx 0$ and $z \approx 1$,³⁸ we combine

³⁷ Tiley et al. (2019) remark that it is difficult to precisely constrain the slope of the Tully–Fisher relation at $z \approx 1$ due to large scatter; they instead perform fixed slope fits to their $z \approx 1$ sample.

³⁸ This lack of evolution in the zero-point is also seen in the baryonic Tully–Fisher relation out to $z = 0.6$ (Puech et al. 2010, 2011) and possibly even to $z = 1.2$ (Weiner et al. 2006).

our modified $v_{\max}-\phi$ relation (Equation (13)) with the $z \approx 0$ K -band absolute magnitude (\mathfrak{M}_K)³⁹ Tully–Fisher relation from Tiley et al. (2019)

$$\mathfrak{M}_K = (-8.3 \pm 0.3) \log \left(\frac{v_{\text{rot}}}{100 \text{ km s}^{-1}} \right) - (22.26 \pm 0.07) \text{ mag}, \quad (16)$$

with $\Delta_{\text{rms}} = 1.17$ mag and $\epsilon = 1.13$ mag, to obtain

$$\mathfrak{M}_K = (7.08 \pm 1.17) [\tan|\phi| - \tan 13^\circ 35'] - (25.03 \pm 0.15) \text{ mag}. \quad (17)$$

This new relation allows us to estimate the intrinsic luminosity of a spiral galaxy (and therefore, a distance) based on its spiral geometry (see van den Bergh 1960a, 1960b, who presented a strong correlation between absolute luminosity and the degree of development of spiral arms), which is measurable from simple imaging.

3.3.1. The $M_{\text{DM}}-\phi$ Relation

Here, we present new evidence that spiral galaxy geometry becomes a useful indicator for the dark matter content of a galaxy. Combining our updated $v_{\max}-\phi$ relation (Equation (13)) with the $M_{\text{DM}}-v_{\max}$ relation (Equation (5)) yields

$$\log \left(\frac{M_{\text{DM}}}{M_\odot} \right) = (-2.08 \pm 0.37) [\tan|\phi| - \tan 13^\circ 35'] + (12.03 \pm 0.11). \quad (18)$$

Adding the total rms scatters from Equations (5) and (13) in quadrature yields an implied $\Delta_{\text{rms}} \simeq 0.25$ dex in the $\log M_{\text{DM}}$ direction. This level of scatter is equivalent to that of the $M_{\star, \text{tot}}-\phi$ relation from Davis et al. (2018), indicating a connection between the large gravitational potential well of a galaxy and its spiral-arm geometry, which is manifest in the $v_{\max}-\phi$ relation (Equation (13)). The ability of ϕ to predict dark matter halo masses in late-type galaxies with such a small slope and level of scatter is remarkable given that no other parameter in this paper is as simple to measure or has such minimal observational requirements.

Mutlu-Pakdil et al. (2018) also presented an $M_{\text{DM}}-\phi$ relation by measuring the pitch angles of spiral galaxies produced from the *Illustris* simulation (Vogelsberger et al. 2014). They found from 95 simulated spiral galaxies that $M_{\text{DM}} \propto (-0.029 \pm 0.001)|\phi|$. When we fit a linear BCES *bisector* regression between M_{DM} and $|\phi|$ for our sample of 42 spiral galaxies, we similarly find $M_{\text{DM}} \propto (-0.028 \pm 0.007)|\phi|$. Therefore, because we find agreement between our observations and the *Illustris* simulations for the $M_{\text{DM}}-\phi$ relation (Equation (18)), but disagree with Mutlu-Pakdil et al. (2018) when it comes to the $M_{\text{BH}}-M_{\text{DM}}$ relation (Equation (12)), we conclude that the *Illustris* simulation (and indeed most simulations) fail to properly model black hole mass scaling relations for spiral galaxies. Specifically, the simulations

appear to correctly model the total stellar mass of spiral galaxies and the corresponding geometry of their spiral arms but underestimate the mass of SMBHs in spiral galaxies.

The existence of an $M_{\text{DM}}-\phi$ relation (Equation (18)) is not unforeseen; the $M_{\text{DM}}-\phi$ and $M_{\text{BH}}-\phi$ relations can be seen as complementary relations to the $M_{\text{BH}}-M_{\text{DM}}$ relation (Equation (12)). Moreover, a correlation has been known to exist between rotation curve shear rate (S)⁴⁰ and spiral-arm pitch angle. Block et al. (1999) and Seigar et al. (2004, 2005, 2006, 2014) have demonstrated the existence of an $S-\phi$ relation from observations, and Grand et al. (2013) have confirmed the correlation through N -body simulations. Precisely, $S = (0.88 \pm 0.08) - (0.014 \pm 0.001)|\phi|$ (Seigar et al. 2006) and $S \simeq 0.85 - 0.014|\phi|$ (Grand et al. 2013).⁴¹

Kalinova et al. (2017) introduced a new parameter to classify the rotation curves of galaxies quantitatively: the coefficient of the first eigenvector (PC_1) of the reconstructed circular velocity rotation curve of a galaxy through principal component analysis.⁴² Yu & Ho (2019) performed an observational study of PC_1 versus $|\phi|$ and uncovered a strong correlation ($r = -0.66$), from which they deduced the implication “that dark matter content might help to shape spiral arms.”

While perhaps not fundamental, ϕ is more a consequence of the presence of a sizeable stabilizing mass, making the disk less self-gravitating. Indeed, when the disk is stable, due to a large central mass (contributed by the bulge and maybe also the dark matter halo), then the pitch angle is small with a tightly wound spiral pattern or even a multi-arm structure. When the disk is unstable, it forms a bar, which can emanate loosely wound spiral arms from its ends. The observational results from Buta et al. (2010a) support this, showing that the frequency of strong bars progressively increases when moving through the morphological types from lenticular to early- and late-type spirals. Additionally, there can be evolution in time because violent bar instability heats the disk, which becomes more stable due to a high Toomre parameter, $Q \equiv \sigma_v / \sigma_{\text{crit}}$, where σ_v is the tangential velocity dispersion and σ_{crit} is the critical (i.e., the minimum dispersion needed for stability) velocity dispersion. Toomre (1964) established that $\sigma_{\text{crit}} \propto \mu / \kappa$, where μ is the disk surface density, and κ is the epicyclic frequency; κ is particularly high when there is a high mass concentration, making σ_{crit} small and the disk stable. In the end, what counts is the mass concentration, not only the bulge (which is part of it). Rotational velocity is also a sign of mass concentration; v_{\max} is higher if the mass is more concentrated for the same total mass.

Numerical simulations also illustrate the importance of mass concentration. A sufficient mass concentration in barred galaxies creates two inner Lindblad resonances, inside of

³⁹ Near-infrared imaging can offer a more complete view of spiral morphology as the optical morphologies of some spiral galaxies can appear significantly different (Block & Wainscoat 1991; Block et al. 1994; Seigar & James 1998a, 1998b), with flocculent optical morphologies occasionally exhibiting grand-design morphologies in the near-infrared (Thornley 1996; Seigar et al. 2003). On the whole, Buta et al. (2010b) found that (save for the most dusty galaxies) $3.6 \mu\text{m}$ morphological classifications are well correlated with blue-light classifications.

⁴⁰ Shear is a dimensionless parameter that quantifies the shape (rising, falling, or flat) of rotation curves, and thus is dependent on the total baryonic and dark matter concentrations. $S = 0.5$ for a flat rotation curve, $S > 0.5$ for a falling rotation curve, and $S < 0.5$ for a rising rotation curve (see Seigar et al. 2014, for a formal definition).

⁴¹ See also the additional studies of the $S-\phi$ relation from simulations (Michikoshi & Kokubo 2014) and observations (Kendall et al. 2015; Yu & Ho 2019). Similarly, Font et al. (2019) conducted a comparison of the “shear parameter” (the difference between the pattern speed of the bar and the spiral arms, relative to the angular rate of the outer disk) versus ϕ in their observational study.

⁴² PC_1 is a measure of the shape and amplitude of the rotation curve and thus reflects the mass distribution of dark matter in galaxies. Galaxies with $\text{PC}_1 > 0$ exhibit high-amplitude centrally peaked rotation curves and galaxies with $\text{PC}_1 < 0$ exhibit low-amplitude slow-rising rotation curves (see Kalinova et al. 2017, for additional information).

which the stable ($\times 2$) periodic prograde orbits⁴³ are perpendicular to the bar and thus do not sustain the bar, but rather weaken it (Shaw et al. 1993). Mayer & Wadsley (2004) showed that bars need a minimum mass to form in galaxies with low surface brightness. Because the disk is diluted and not self-gravitating in a stabilizing halo, this leads to multi-arm or tightly wound spiral patterns with small $|\phi|$. Foyle et al. (2008) demonstrated how the mass concentration can change the pattern and also create two exponential disks.

A decade of research has demonstrated a strong correlation between pitch angle and black hole mass (Seigar et al. 2008; Ringermacher & Mead 2009; Berrier et al. 2013; Davis et al. 2017). Combining the fact that the geometry of spiral arms is undeniably a consequence of galactic rotation (and likely other factors such as the bulge mass and the density of the disk, see Davis et al. 2015) with the results of these aforementioned studies of M_{DM} , M_{BH} , ϕ , and shear, inevitably lead to the conclusion that an $M_{\text{DM}}-\phi$ relation must exist. Notably, the total gravitational mass of a galaxy determines its $v_{\text{rot}}(R)$ profile, shear rate is a parameterization of the differential rotation exhibited by the $v_{\text{rot}}(R)$ profile, which establishes a quasi-static density wave and generates a long-lived logarithmic spiral pattern of enhanced star formation with a unique pitch angle.

Moving farther afield, high- z spirals are rare but documented in the literature. Labbé et al. (2003) presented a sample of half a dozen “large disk-like galaxies at high redshift” ($1.4 \leq z \leq 3.0$), with some of the nearer galaxies exhibiting “evidence of well-developed grand-design spiral structure.” Contini et al. (2016) studied a sample of 28 star-forming galaxies at $0.2 < z < 1.4$, some of which were identified to exhibit spiral structure. Similarly, Burkert et al. (2016) analyzed a sample of 433 ($0.76 < z < 2.6$) massive star-forming disk galaxies. Recently, Yuan et al. (2017) discovered a gravitationally lensed high-redshift spiral galaxy at $z = 2.54$ through source-plane reconstruction, making it “the highest-redshift spiral galaxy observed with the highest spatial resolution and spectroscopic depth to date.”⁴⁴ Just a few years ago, spiral galaxies were thought not to exist beyond $z \sim 1.8$, and the spirals found at $z \gtrsim 1$ were thought not to be true spirals, merely “spiral-like alignments of star formation clumps” (Elmegreen & Elmegreen 2014). Studies of these early epochs are essential for evolutionary studies. van Dokkum et al. (2013) showed that mass growth in the central regions (and the black holes) of present-day Milky Way-like galaxies occurred primarily between $z = 2.5$ and $z = 1$.

The discovery of high- z spiral galaxies allows for the derivation of the high- z $v_{\text{max}}-\phi$ and high- z $v_{\text{max}}-\sigma_0$ relations, which can be compared with their local counterparts, checking for signs of evolution. There may also be implications for the evolution of the black hole mass. Recent results from Drew et al. (2018) reveal a star-bursting galaxy at $z = 1.6$ with a flat outer rotation curve, which is indicative of a rotation-supported disk galaxy, rich in dark matter and similar to disk galaxies at low redshift. If this single finding is representative of other high- z galaxies, our $M_{\text{DM}}-\phi$ relation may become a useful tool in the estimation of dark matter at earlier epochs than our local sample. Because logarithmic spirals are scale-invariant curves

and are thus unaltered by distance, ϕ might be an ideal messenger to convey an estimate of a host galaxy dark matter mass, especially at high redshifts, if the $M_{\text{DM}}-\phi$ relation does not evolve with z , and we can therefore use the local $M_{\text{DM}}-\phi$ relation.

4. Conclusions

The $v_{\text{max}}-\sigma_0$ relation (Section 3.1) provides insights into the apparent connection between the kinematics of a galaxy dark matter halo and its stellar bulge. We have shown that the $v_{\text{max}}-\sigma_0$ relation, for $\sigma_0 \gtrsim 100 \text{ km s}^{-1}$, is consistent with studies over nearly the past two decades. We find that the slope is inconsistent with a value of one at the 3.5σ level, revealing that v_{max}/σ_0 is not a constant value. We introduce and highlight the implied $M_{\text{DM}}-\sigma_0$ relation (Equation (8)) and its practical application for galaxies with σ_0 measurements of their bulges, yielding predictions of their dark matter halo masses.

We have presented observational evidence that a strong correlation exists between M_{BH} and v_{max} for spiral galaxies (Figure 2). The $M_{\text{BH}}-v_{\text{max}}$ and $M_{\text{BH}}-\sigma_0$ relations for spiral galaxies with $\sigma_0 \gtrsim 100 \text{ km s}^{-1}$ have similar levels of scatter, with $\Delta_{\text{rms}} = 0.58 \text{ dex}$ and 0.63 dex in $\log M_{\text{BH}}$, respectively. Alleged pseudobulges dominate our sample of spiral galaxies (36 out of 42). Some may therefore prefer v_{max} over σ_0 as a predictor of black hole masses for spiral galaxies. Our $M_{\text{BH}}-v_{\text{max}}$ relation (Equation (10)) is steeper than previous studies, but we argue that past studies did not demonstrate consistency between complementary scaling relations, i.e., the slope we present for the $M_{\text{BH}}-v_{\text{max}}$ relation is supported by its agreement with the unification of the Tully-Fisher ($M_{\text{BH}}-v_{\text{max}}$) relation (Equation (1)) and the $M_{\text{BH}}-M_{\text{DM}}$ relation (Equation (2)).

The scatter for the $M_{\text{BH}}-M_{\text{DM}}$ relation (Davis et al. 2018) is higher ($\Delta_{\text{rms}} = 0.79 \text{ dex}$ in $\log M_{\text{BH}}$), suggesting that the influence of dark matter, as traced by v_{max} ,⁴⁵ (rather than total stellar mass) on the central black hole mass is relevant. The low Δ_{rms} value of just 0.43 dex in $\log M_{\text{BH}}$ (Davis et al. 2017) about the shallow slope of the $M_{\text{BH}}-\phi$ relation still remains unmatched for spiral galaxies via ϕ , which is a defining characteristic of spiral galaxies. We acknowledge that these studies (i.e., Davis et al. 2017, 2018, 2019, and this work) focus on a sample constructed from selection of all spiral galaxies with available dynamical mass estimates of their central black holes. Because the sample size (48) is not yet large enough to explore a volume-limited sample, the resulting scaling relations unavoidably suffer from selection effects. Thus, underrepresented populations of galaxies with difficult to measure black hole masses would likely act to increase the scatter in these relations if they could be included (i.e., the quoted scatters should be considered minimum estimates),

Because v_{max} is a reliable predictor of M_{DM} for late-type galaxies (Katz et al. 2018b), our strong $M_{\text{BH}}-v_{\text{max}}$ correlation ($r = 0.74$ and $r_s = 0.72$) retains its strength when translated into an $M_{\text{BH}}-M_{\text{DM}}$ relation (Equation (12)). We find steep slopes for these two relations, which is indicative of a history of substantial black hole mass increase through accretion and long-lived quasars (Haehnelt et al. 1998). Concerning late-type galaxies, evolution along the steep $M_{\text{BH}}-M_{\text{DM}}^{3.05 \pm 0.53}$ relation

⁴³ For supplementary reading on families of periodic orbits, see Contopoulos & Papayannopoulos (1980), Contopoulos & Grosbol (1989), Sellwood & Wilkinson (1993), Binney & Tremaine (2011), and Sellwood (2014).

⁴⁴ See also the potential evidence for spiral arms in high-redshift submillimeter galaxies from Hodge et al. (2018).

⁴⁵ All relations in this work involving M_{DM} are constrained by the Di Cintio et al. (2014a) halo profile and the empirical $M_{\text{DM}}-v_{\text{max}}$ relation (Equation (5)) of Katz et al. (2018b). Other relations using v_{max} are based directly on observational data.

implies that galaxies host black holes that underwent rapid mass growth relative to their host (i.e., relative to maintaining a constant $M_{\text{BH}}/M_{*,\text{tot}}$ ratio). We echo our arguments from Davis et al. (2018) that it is crucial to separate galaxies according to morphology when black hole mass scaling relations are investigated. As revealed in Savorgnan et al. (2016) and Sahu et al. (2019), the $M_{\text{BH}}-M_{*,\text{tot}}$ relation for early-type galaxies is very different.

We have also provided evidence of a link between the geometry of spiral galaxy arms and their dark matter halos. Indeed, the seminal work by Kennicutt (1981) qualitatively showed that v_{max} is well correlated with ϕ , in particular for the later-type spiral galaxies. Such a specific connection between the kinematics of a galaxy and its spiral pattern has important consequences for spiral-arm genesis theories, such as the spiral density-wave (quasi-stationary spiral structure) modal theory (Lindblad 1963, 1964; Lin & Shu 1964, 1966; Roberts et al. 1975; Roberts 1975; Bertin et al. 1989a, 1989b; Bertin 1991, 1993, 1996; Fuchs 1991, 2000; Bertin & Lin 1996), swing amplification theory (Julian & Toomre 1966; Goldreich & Tremaine 1978; Toomre 1981; Toomre & Kalnajs 1991; D’Onghia et al. 2013), kinematic spiral waves (Kalnajs 1973; Toomre 1977), the stochastic self-propagating star formation theory (Gerola & Seiden 1978; Seiden & Gerola 1979), solid-body rotation of material arms (Kormendy & Norman 1979), recurrent cycles of groove modes (Sellwood 2000), manifold theory (Romero-Gómez et al. 2006; Voglis et al. 2006b, see also Danby 1965),⁴⁶ superposed transient instabilities (Sellwood & Carlberg 2014), etc. We have quantified the $v_{\text{max}}-\phi$ relation (Equation (13)) to enable and facilitate testing between rival theories of spiral-arm formation (Kennicutt & Hodge 1982). The connection between spiral-arm winding and kinematics can also be applied to the Tully–Fisher relation to indirectly estimate distances to spiral galaxies (Equation (17)). For a complete understanding of galaxy formation and evolutionary processes, it is necessary to study and gain insight into the influence of dark matter. To that end, we have translated the $v_{\text{max}}-\phi$ relation into an $M_{\text{DM}}-\phi$ relation (Equation (18)) providing for the first time a useful method of predicting dark matter halo masses from the geometry of spiral arms in uncalibrated photometric images of spiral galaxies.

Metaphorically, we can ascribe a dark matter halo as the central nervous system of its host galaxy, filling and connecting all regions of the galaxy. Indeed, the dark matter halo of a spiral galaxy can be considered a legitimate puppet-master, covertly influencing the observable properties and components of its host galaxy. This notion that the dark matter halo determines everything in a spiral galaxy (e.g., v_{max} , mass concentration, and maybe M_{BH}) has already been put forward by the proponents of modified gravity (Milgrom 1983; McGaugh et al. 2000): when the baryon distribution is known, the implied dark matter distribution and total mass can be deduced.⁴⁷ Much of this dates back to the Tully–Fisher relation (Tully & Fisher 1977; Aaronson et al. 1979, 1980; Mould et al. 1980; Aaronson & Mould 1983), refined by the baryonic

Tully–Fisher relation (Freeman 1999; Walker 1999; McGaugh et al. 2000).⁴⁸

Intermediate-mass black holes (IMBHs; $10^2 M_{\odot} \leq M_{\text{BH}} < 10^5 M_{\odot}$) remain elusive stepping stones in the evolution from stellar mass ($M_{\text{BH}} < 10^2 M_{\odot}$) to supermassive ($M_{\text{BH}} \geq 10^5 M_{\odot}$) black holes (see Mezcua 2017 and Koliopanos 2017 for reviews). Recent studies (Koliopanos et al. 2017; Graham & Soria 2019; Graham et al. 2019) have used multiple black hole mass scaling relations, in combination with X-ray observations of nuclear point sources, to identify IMBH candidates in local galaxies. Studies like these provide several independent estimates of black hole masses and serve as important guides for follow-up targets to hopefully confirm IMBH masses through more direct measurements. We offer one additional black hole mass scaling relation: $M_{\text{BH}}-v_{\text{max}}$, which, when extrapolated, predicts that galaxies with $v_{\text{max}} < 130 \text{ km s}^{-1}$ ($\log [M_{\text{DM}}/M_{\odot}] < 11.49$ through Equation (12)) should harbor IMBHs. For reference, our Galaxy⁴⁹ has $v_{\text{max}} = (198 \pm 6) \text{ km s}^{-1}$ and $\log (M_{\text{DM}}/M_{\odot}) = 11.86 \pm 0.01$ (Eilers et al. 2019), with $\log (M_{\text{BH}}/M_{\odot}) = 6.60 \pm 0.02$ (Boehle et al. 2016).

Despite claims that M_{BH} does not correlate with disks (Kormendy et al. 2011), the $M_{\text{BH}}-v_{\text{max}}$ relation for spiral galaxies has similar scatter as the $M_{\text{BH}}-\sigma_0$ relation for spiral galaxies with $\sigma_0 \gtrsim 100 \text{ km s}^{-1}$. The steep $M_{\text{BH}}-v_{\text{max}}$ relation observed here brings consistency between the Tully–Fisher relation ($M_{*,\text{tot}} \propto v_{\text{rot}}^{4.0 \pm 0.1}$) and the $M_{\text{BH}} \propto M_{*,\text{tot}}^{3.05 \pm 0.53}$ relation for spiral galaxies. We note that the $M_{\text{BH}}-v_{\text{max}}$ relation (Equation (10)) and the $v_{\text{max}}-\sigma_0$ relation (Equation (6)) are also compatible with the $M_{\text{BH}}-\sigma_0$ relation for spiral galaxies (Davis et al. 2017), i.e., $M_{\text{BH}} \propto v_{\text{max}}^{10.62 \pm 1.37}$ combined with $v_{\text{max}}-\sigma_0^{0.65 \pm 0.10}$ yields $M_{\text{BH}} \propto \sigma_0^{6.87 \pm 1.42}$, which is consistent with our result for spiral galaxies ($M_{\text{BH}} \propto \sigma_0^{5.65 \pm 0.79}$) from Davis et al. (2017) at the level of 0.55 σ . Alternatively, if we cautiously assume that a selection bias is present, censoring galaxies with low σ_0 from our sample, we can instead combine Equation (10) with Equation (7), which yields $M_{\text{BH}} \propto \sigma_0^{3.21 \pm 1.19}$. When we compare this with the (Y|X) regression fit to the $M_{\text{BH}}-\sigma_0$ relation (which similarly reduces any potential bias due to unobserved galaxies with low velocity dispersions) from Davis et al. (2017), $M_{\text{BH}} \propto \sigma_0^{3.88 \pm 0.89}$, there is consistency at the level of 0.32 σ . To conclude, the self-consistent relations presented in this work were derived from a spiral galaxy sample with directly measured SMBH masses that doubles the size of previous samples. These relations necessitate a salient revision to constraints that are applied to theory and simulations.

We thank Duncan Forbes and Victor Debattista for feedback that helped improve the presentation of this paper. The Australian Research Council’s funding scheme DP17012923 supported A.W.G. Parts of this research were conducted by the Australian Research Council Centre of Excellence for Gravitational Wave Discovery (OzGrav), through project number CE170100004. This research has made use of NASA’s Astrophysics Data System. We acknowledge use of the HyperLeda database (<http://leda.univ-lyon1.fr>).




⁴⁶ Two versions of the manifold theory have been developed: (i) the “flux-tube” version (Romero-Gómez et al. 2006, 2007; Athanassoula et al. 2009a, 2009b, 2010; Athanassoula 2012) and (ii) the “apocentric manifolds” version (Voglis et al. 2006a, 2006b; Tsoutsis et al. 2008, 2009; Efthymiopoulos 2010; Harsoula et al. 2016); see also the recent work by Efthymiopoulos et al. (2019).

⁴⁷ From the standpoint of modified Newtonian dynamics, Milgrom (1983) would argue that the baryonic mass is the total mass (i.e., there is no dark matter).

⁴⁸ This critical dependency on the inventory of baryons would also necessitate an accounting of the gas in galaxies as well (i.e., taking gas into account should improve all scaling relations). For our sample, the gas content is thought to be a small fraction of the total mass, and thus we ignore it.

⁴⁹ The quantity v_{max} should not be confused with the circular rotation velocity of the disk of our Galaxy at the location of the Sun and equal to $(238 \pm 15) \text{ km s}^{-1}$ (Bland-Hawthorn & Gerhard 2016) or $(229.0 \pm 0.2) \text{ km s}^{-1}$ (Eilers et al. 2019).

ORCID iDs

Benjamin L. Davis  <https://orcid.org/0000-0002-4306-5950>
 Alister W. Graham  <https://orcid.org/0000-0002-6496-9414>
 Françoise Combes  <https://orcid.org/0000-0003-2658-7893>

References

- Aaronson, M., Huchra, J., & Mould, J. 1979, *ApJ*, **229**, 1
 Aaronson, M., & Mould, J. 1983, *ApJ*, **265**, 1
 Aaronson, M., Mould, J., Huchra, J., et al. 1980, *ApJ*, **239**, 12
 Adams, F. C., Graff, D. S., & Richstone, D. O. 2001, *ApJL*, **551**, L31
 Akerib, D. S., Alsum, S., Araújo, H. M., et al. 2017, *PhRvL*, **118**, 021303
 Akritas, M. G., & Bershadsky, M. A. 1996, *ApJ*, **470**, 706
 Alexander, T. 2005, *PhR*, **419**, 65
 Alloin, D., Pelat, D., Phillips, M., & Whittle, M. 1985, *ApJ*, **288**, 205
 Amorim, A., Bauböck, M., Berger, J. P., et al. 2019, *PhRvL*, **122**, 101102
 Aprile, E., Aalbers, J., Agostini, F., et al. 2018, *PhRvL*, **121**, 111302
 Araya Salvo, C., Mathur, S., Ghosh, H., Fiore, F., & Ferrarese, L. 2012, *ApJ*, **757**, 179
 Arcadi, G., Dutra, M., Ghosh, P., et al. 2018, *EPJC*, **78**, 203
 Artale, M. C., Pedrosa, S. E., Tissera, P. B., Cataldi, P., & Di Cintio, A. 2019, *A&A*, **622**, A197
 Athanassoula, E. 2002, *ApJL*, **569**, L83
 Athanassoula, E. 2012, *MNRAS*, **426**, L46
 Athanassoula, E., Laurikainen, E., Salo, H., & Bosma, A. 2015, *MNRAS*, **454**, 3843
 Athanassoula, E., Romero-Gómez, M., Bosma, A., & Masdemont, J. J. 2009a, *MNRAS*, **400**, 1706
 Athanassoula, E., Romero-Gómez, M., Bosma, A., & Masdemont, J. J. 2010, *MNRAS*, **407**, 1433
 Athanassoula, E., Romero-Gómez, M., & Masdemont, J. J. 2009b, *MNRAS*, **394**, 67
 Athanassoula, E. 2016, in *Galactic Bulges, Astrophysics and Space Science Library*, Vol. 418, ed. E. Laurikainen, R. Peletier, & D. Gadotti (Cham: Springer International), 391
 Babcock, H. W. 1939, *LicOB*, **19**, 41
 Baes, M., Buyle, P., Hau, G. K. T., & Dejonghe, H. 2003, *MNRAS*, **341**, L44
 Bandara, K., Crampton, D., & Simard, L. 2009, *ApJ*, **704**, 1135
 Bardeen, J. M., Press, W. H., & Teukolsky, S. A. 1972, *ApJ*, **178**, 347
 Bassett, R., Glazebrook, K., Fisher, D. B., et al. 2014, *MNRAS*, **442**, 3206
 Batcheldor, D. 2010, *ApJL*, **711**, L108
 Beckwith, S. V. W., Stiavelli, M., Koekemoer, A. M., et al. 2006, *AJ*, **132**, 1729
 Behroozi, P., Wechsler, R., Hearin, A., & Conroy, C. 2019, *MNRAS*, in press (doi:10.1093/mnras/stz1182)
 Behroozi, P. S., Conroy, C., & Wechsler, R. H. 2010, *ApJ*, **717**, 379
 Behroozi, P. S., Wechsler, R. H., & Conroy, C. 2013, *ApJ*, **770**, 57
 Beifiori, A., Courteau, S., Corsini, E. M., & Zhu, Y. 2012, *MNRAS*, **419**, 2497
 Beifiori, A., Sarzi, M., Corsini, E. M., et al. 2009, *ApJ*, **692**, 856
 Bellovary, J. M., Holley-Bockelmann, K., Gültekin, K., et al. 2014, *MNRAS*, **445**, 2667
 Berrier, J. C., Davis, B. L., Kenefick, D., et al. 2013, *ApJ*, **769**, 132
 Bertin, G. 1991, in *IAU Symp. 146, Dynamics of Galaxies and Their Molecular Cloud Distributions*, ed. F. Combes & F. Casoli (Dordrecht: Kluwer Academic), 93
 Bertin, G. 1993, *PASP*, **105**, 640
 Bertin, G. 1996, in *New Extragalactic Perspectives in the New South Africa, Astrophysics and Space Science Library*, Vol. 209, ed. D. L. Block & J. M. Greenberg (Dordrecht: Kluwer Academic), 227
 Bertin, G., & Lin, C. C. 1996, *Spiral Structure in Galaxies a Density Wave Theory* (Cambridge, MA: MIT Press)
 Bertin, G., Lin, C. C., Lowe, S. A., & Thurstans, R. P. 1989a, *ApJ*, **338**, 78
 Bertin, G., Lin, C. C., Lowe, S. A., & Thurstans, R. P. 1989b, *ApJ*, **338**, 104
 Bezanson, R., van Dokkum, P. G., Franx, M., et al. 2011, *ApJL*, **737**, L31
 Binney, J., & Tremaine, S. 2011, *Galactic Dynamics* (2nd ed.; Princeton, NJ: Princeton Univ. Press)
 Birrer, S., Lilly, S., Amara, A., Paranjape, A., & Refregier, A. 2014, *ApJ*, **793**, 12
 Bland-Hawthorn, J., & Gerhard, O. 2016, *ARA&A*, **54**, 529
 Block, D. L., Bertin, G., Stockton, A., et al. 1994, *A&A*, **288**, 365
 Block, D. L., Puerari, I., Frogel, J. A., et al. 1999, *Ap&SS*, **269**, 5
 Block, D. L., & Wainscoat, R. J. 1991, *Natur*, **353**, 48
 Boehle, A., Ghez, A. M., Schödel, R., et al. 2016, *ApJ*, **830**, 17
 Bogdán, Á., & Goulding, A. D. 2015, *ApJ*, **800**, 124
 Booth, C. M., & Schaye, J. 2010, *MNRAS*, **405**, L1
 Bosma, A. 1981, *AJ*, **86**, 1791
 Bosma, A. 1996, in *ASP Conf. Ser. 91, IAU Coll. 157: Barred Galaxies*, ed. R. Buta, D. A. Crocker, & B. G. Elmegreen (San Francisco, CA: ASP), 132
 Broeils, A. H. 1992, *A&A*, **256**, 19
 Brown, J. S., Valluri, M., Shen, J., & Debattista, V. P. 2013, *ApJ*, **778**, 151
 Burbidge, E. M., & Burbidge, G. R. 1959, *ApJ*, **130**, 20
 Bureau, M., & Freeman, K. C. 1999, *AJ*, **118**, 126
 Burkert, A., & Forbes, D. 2019, arXiv:1901.00900
 Burkert, A., Förster Schreiber, N. M., Genzel, R., et al. 2016, *ApJ*, **826**, 214
 Buta, R., Laurikainen, E., Salo, H., & Knapen, J. H. 2010a, *ApJ*, **721**, 259
 Buta, R. J., Corwin, H. G., & Odewahn, S. C. 2007, *The de Vaucouleurs Atlas of Galaxies* (Cambridge: Cambridge Univ. Press)
 Buta, R. J., Sheth, K., Athanassoula, E., et al. 2015, *ApJS*, **217**, 32
 Buta, R. J., Sheth, K., Regan, M., et al. 2010b, *ApJS*, **190**, 147
 Cattaneo, A., Haehnelt, M. G., & Rees, M. J. 1999, *MNRAS*, **308**, 77
 Ciambur, B. C., & Graham, A. W. 2016, *MNRAS*, **459**, 1276
 Cisternas, M., Jahnke, K., Inskip, K. J., et al. 2011, *ApJ*, **726**, 57
 Combes, F., Debbasch, F., Friedli, D., & Pfenniger, D. 1990, *A&A*, **233**, 82
 Combes, F., García-Burillo, S., Audibert, A., et al. 2019, *A&A*, **623**, A79
 Contini, T., Epinat, B., Bouché, N., et al. 2016, *A&A*, **591**, A49
 Contopoulos, G., & Grosbol, P. 1989, *A&ARv*, **1**, 261
 Contopoulos, G., & Papayannopoulos, T. 1980, *A&A*, **92**, 33
 Costantin, L., Corsini, E. M., Méndez-Abreu, J., et al. 2018, *MNRAS*, **481**, 3623
 Courteau, S., Andersen, D. R., Bershadsky, M. A., MacArthur, L. A., & Rix, H.-W. 2003, *ApJ*, **594**, 208
 Courteau, S., McDonald, M., Widrow, L. M., & Holtzman, J. 2007, *ApJL*, **655**, L21
 Courtois, H. M., Tully, R. B., Fisher, J. R., et al. 2009, *AJ*, **138**, 1938
 Cowsik, R., & McClelland, J. 1972, *PhRvL*, **29**, 669
 Cresci, G., Hicks, E. K. S., Genzel, R., et al. 2009, *ApJ*, **697**, 115
 Danby, J. M. A. 1965, *AJ*, **70**, 501
 Danver, C.-G. 1942, *AnLun*, **10**, 3
 Davis, B. L., Berrier, J. C., Johns, L., et al. 2014, *ApJ*, **789**, 124
 Davis, B. L., Berrier, J. C., Shields, D. W., et al. 2012, *ApJS*, **199**, 33
 Davis, B. L., Berrier, J. C., Shields, D. W., et al. 2016, 2DFFT: Measuring Galactic Spiral Arm Pitch Angle, *Astrophysics Source Code Library*, ascl:1608.015
 Davis, B. L., Graham, A. W., & Cameron, E. 2018, *ApJ*, **869**, 113
 Davis, B. L., Graham, A. W., & Cameron, E. 2019, *ApJ*, **873**, 85
 Davis, B. L., Graham, A. W., & Seigar, M. S. 2017, *MNRAS*, **471**, 2187
 Davis, B. L., Kenefick, D., Kenefick, J., et al. 2015, *ApJL*, **802**, L13
 Davis, D. R., & Hayes, W. B. 2014, *ApJ*, **790**, 87
 Debattista, V. P., Kazantzidis, S., & van den Bosch, F. C. 2013, *ApJ*, **765**, 23
 de Blok, W. J. G., & Bosma, A. 2002, *A&A*, **385**, 816
 de Blok, W. J. G., McGaugh, S. S., Bosma, A., & Rubin, V. C. 2001, *ApJL*, **552**, L23
 Debuhr, J., Quataert, E., Ma, C.-P., & Hopkins, P. 2010, *MNRAS*, **406**, L55
 de Vaucouleurs, G. 1974, in *IAU Symp. 58, The Formation and Dynamics of Galaxies*, ed. J. R. Shakeshaft (Dordrecht: Reidel), 335
 Di Cintio, A., Brook, C. B., Dutton, A. A., et al. 2014a, *MNRAS*, **441**, 2986
 Di Cintio, A., Brook, C. B., Macciò, A. V., et al. 2014b, *MNRAS*, **437**, 415
 Di Matteo, T., Croft, R. A. C., Springel, V., & Hernquist, L. 2003, *ApJ*, **593**, 56
 Dobbs, C., & Baba, J. 2014, *PASA*, **31**, e035
 D'Onghia, E., Vogelsberger, M., & Hernquist, L. 2013, *ApJ*, **766**, 34
 Drew, P. M., Casey, C. M., Burnham, A. D., et al. 2018, *ApJ*, **869**, 58
 Du, M., Debattista, V. P., Shen, J., Ho, L. C., & Erwin, P. 2017, *ApJL*, **844**, L15
 Efthymiopoulos, C. 2010, *EPJST*, **186**, 91
 Efthymiopoulos, C., Kyziroopoulos, P. E., Páez, R. I., Zouloumi, K., & Gravanis, G. A. 2019, *MNRAS*, **484**, 1487
 Eilers, A.-C., Hogg, D. W., Rix, H.-W., & Ness, M. K. 2019, *ApJ*, **871**, 120
 Einstein, A. 1916, *AnP*, **354**, 769
 Elmegreen, D. M., & Elmegreen, B. G. 2014, *ApJ*, **781**, 11
 Emsellem, E., Cappellari, M., Krajnović, D., et al. 2011, *MNRAS*, **414**, 888
 Erroz-Ferrer, S., Knapen, J. H., Leaman, R., et al. 2015, *MNRAS*, **451**, 1004
 Erwin, P., & Debattista, V. P. 2013, *MNRAS*, **431**, 3060
 Event Horizon Telescope Collaboration, Akiyama, K., Alberdi, A., et al. 2019, *ApJL*, **875**, L1
 Evrard, A. E., Bialek, J., Busha, M., et al. 2008, *ApJ*, **672**, 122
 Ferguson, H. C., Dickinson, M., & Williams, R. 2000, *ARA&A*, **38**, 667
 Ferrarese, L. 2002, *ApJ*, **578**, 90
 Ferrarese, L., & Ford, H. 2005, *SSRV*, **116**, 523

- Fisher, D. B., & Drory, N. 2016, *Galactic Bulges*, 418, 41
- Flores, R., Primack, J. R., Blumenthal, G. R., & Faber, S. M. 1993, *ApJ*, 412, 443
- Font, J., Beckman, J. E., James, P. A., & Patsis, P. A. 2019, *MNRAS*, 482, 5362
- Foyle, K., Courteau, S., & Thacker, R. J. 2008, *MNRAS*, 386, 1821
- Freeman, K. C. 1970, *ApJ*, 160, 811
- Freeman, K. C. 1999, in ASP Conf. Ser. 170, *The Low Surface Brightness Universe*, ed. J. I. Davies, C. Impey, & S. Phillips (San Francisco, CA: ASP), 3
- Fuchs, B. 1991, in *Dynamics of Disk Galaxies*, ed. B. Sundelius (Göteborg: Chalmers Univ. of Technology), 359
- Fuchs, B. 2000, in ASP Conf. Ser. 197, *Dynamics of Galaxies: from the Early Universe to the Present*, ed. F. Combes, G. A. Mamon, & V. Charmandaris (San Francisco, CA: ASP), 53
- Gadotti, D. A., & Sánchez-Janssen, R. 2012, *MNRAS*, 423, 877
- García-Rissmann, A., Vega, L. R., Asari, N. V., et al. 2005, *MNRAS*, 359, 765
- Gentile, G., Salucci, P., Klein, U., Vergani, D., & Kalberla, P. 2004, *MNRAS*, 351, 903
- Genzel, R., Eisenhauer, F., & Gillessen, S. 2010, *RvMP*, 82, 3121
- Gerola, H., & Seiden, P. E. 1978, *ApJ*, 223, 129
- Gershtein, S. S., & Zel'dovich, Y. B. 1966, *ZhPmR*, 4, 174
- Goldreich, P., & Tremaine, S. 1978, *ApJ*, 222, 850
- Gorski, M., Ott, J., Rand, R., et al. 2018, *ApJ*, 856, 134
- Graham, A. 2015, *HiA*, 16, 360
- Graham, A. W. 2016, *Galactic Bulges*, 418, 263
- Graham, A. W., & Driver, S. P. 2007, *ApJ*, 655, 77
- Graham, A. W., Driver, S. P., Allen, P. D., & Liske, J. 2007, *MNRAS*, 378, 198
- Graham, A. W., Onken, C. A., Athanassoula, E., & Combes, F. 2011, *MNRAS*, 412, 2211
- Graham, A. W., & Soria, R. 2019, *MNRAS*, 484, 794
- Graham, A. W., Soria, R., & Davis, B. L. 2019, *MNRAS*, 484, 814
- Grand, R. J. J., Kawata, D., & Cropper, M. 2013, *A&A*, 553, A77
- Gravity Collaboration, Abuter, R., Amorim, A., et al. 2018a, *A&A*, 615, L15
- Gravity Collaboration, Abuter, R., Amorim, A., et al. 2018b, *A&A*, 618, L10
- Green, A. W., Glazebrook, K., McGregor, P. J., et al. 2010, *Natur*, 467, 684
- Green, A. W., Glazebrook, K., McGregor, P. J., et al. 2014, *MNRAS*, 437, 1070
- Groot, H. 1925, *MNRAS*, 85, 535
- Haehnelt, M. G., & Kauffmann, G. 2000, *MNRAS*, 318, L35
- Haehnelt, M. G., Natarajan, P., & Rees, M. J. 1998, *MNRAS*, 300, 817
- Hansen, S. M., Sheldon, E. S., Wechsler, R. H., & Koester, B. P. 2009, *ApJ*, 699, 1333
- Harris, C. E., Bennert, V. N., Auger, M. W., et al. 2012, *ApJS*, 201, 29
- Harsoula, M., Efthymiopoulos, C., & Contopoulos, G. 2016, *MNRAS*, 459, 3419
- Hartmann, M., Debattista, V. P., Cole, D. R., et al. 2014, *MNRAS*, 441, 1243
- Hasan, F., & Crocker, A. 2019, arXiv:1904.00486
- Haynes, M. P., Giovanelli, R., Kent, B. R., et al. 2018, *ApJ*, 861, 49
- Herrera-Endoqui, M., Salo, H., Laurikainen, E., & Knapen, J. H. 2017, *A&A*, 599, A43
- Ho, L. C. 2007, *ApJ*, 668, 94
- Hodge, J. A., Smail, I., Walter, F., et al. 2018, *ApJ*, in press (arXiv:1810.12307)
- Hooper, D. 2018, arXiv:1812.02029
- Hopkins, P. F., & Quataert, E. 2010, *MNRAS*, 407, 1529
- Illingworth, G. 1983, in *IAU Symp. 100, Internal Kinematics and Dynamics of Galaxies*, ed. E. Athanassoula (Dordrecht: D. Reidel), 257
- Issaoun, S., Johnson, M. D., Blackburn, L., et al. 2019, *ApJ*, 871, 30
- Izquierdo-Villalba, D., Bonoli, S., Spinoso, D., et al. 2019, arXiv:1901.10490
- Jarvis, B. J. 1986, *AJ*, 91, 65
- Jeans, J. H. 1922, *MNRAS*, 82, 122
- Jiang, Y.-F., Greene, J. E., Ho, L. C., Xiao, T., & Barth, A. J. 2011, *ApJ*, 742, 68
- Julian, W. H., & Toomre, A. 1966, *ApJ*, 146, 810
- Kalinova, V., Colombo, D., Rosolowsky, E., et al. 2017, *MNRAS*, 469, 2539
- Kalnajs, A. J. 1973, *PASAu*, 2, 174
- Kang, W.-R., Woo, J.-H., Schulze, A., et al. 2013, *ApJ*, 767, 26
- Kapteyn, J. C. 1922, *ApJ*, 55, 302
- Katz, H., Desmond, H., Lelli, F., et al. 2018a, *MNRAS*, 480, 4287
- Katz, H., Desmond, H., McGaugh, S., & Lelli, F. 2018b, *MNRAS*, 483, L98
- Katz, H., Lelli, F., McGaugh, S. S., et al. 2017, *MNRAS*, 466, 1648
- Kendall, S., Clarke, C., & Kennicutt, R. C. 2015, *MNRAS*, 446, 4155
- Kendall, S., Kennicutt, R. C., & Clarke, C. 2011, *MNRAS*, 414, 538
- Kennicutt, R. C. J. 1981, *AJ*, 86, 1847
- Kennicutt, R. J., & Hodge, P. 1982, *ApJ*, 253, 101
- Kerr, R. P. 1963, *PhRvL*, 11, 237
- Kocevski, D. D., Faber, S. M., Mozena, M., et al. 2012, *ApJ*, 744, 148
- Koliopoulos, F. 2017, in *Proc. XII Multifrequency Behaviour of High Energy Cosmic Sources Workshop (Trieste: SISSA)*, 51
- Koliopoulos, F., Ciambur, B. C., Graham, A. W., et al. 2017, *A&A*, 601, A20
- Kormendy, J., & Bender, R. 2011, *Natur*, 469, 377
- Kormendy, J., Bender, R., & Cornell, M. E. 2011, *Natur*, 469, 374
- Kormendy, J., & Norman, C. A. 1979, *ApJ*, 233, 539
- Kormendy, J., & Richstone, D. 1995, *ARA&A*, 33, 581
- Kornei, K. A., & McCrady, N. 2009, *ApJ*, 697, 1180
- Krajnović, D., Emsellem, E., Cappellari, M., et al. 2011, *MNRAS*, 414, 2923
- Kravtsov, A. V., Vikhlinin, A. A., & Meshcheryakov, A. V. 2018, *AsTL*, 44, 8
- Krumm, N., & Salpeter, E. E. 1979, *AJ*, 84, 1138
- Kuzio de Naray, R., McGaugh, S. S., & de Blok, W. J. G. 2008, *ApJ*, 676, 920
- Kuzio de Naray, R., McGaugh, S. S., de Blok, W. J. G., & Bosma, A. 2006, *ApJS*, 165, 461
- Kuzio de Naray, R., McGaugh, S. S., & Mihos, J. C. 2009, *ApJ*, 692, 1321
- Labbé, I., Rudnick, G., Franx, M., et al. 2003, *ApJL*, 591, L95
- Laurikainen, E., & Salo, H. 2016, in *Galactic Bulges, Astrophysics and Space Science Library*, Vol. 418, ed. E. Laurikainen, R. Peletier, & D. Gadotti (Cham: Springer International), 77
- Laurikainen, E., & Salo, H. 2017, *A&A*, 598, A10
- Laurikainen, E., Salo, H., Athanassoula, E., et al. 2013, *MNRAS*, 430, 3489
- Laurikainen, E., Salo, H., Athanassoula, E., Bosma, A., & Herrera-Endoqui, M. 2014, *MNRAS*, 444, L80
- Laurikainen, E., Salo, H., Buta, R., & Knapen, J. 2015, *HiA*, 16, 331
- Laurikainen, E., Salo, H., Buta, R., & Knapen, J. H. 2011, *MNRAS*, 418, 1452
- Laurikainen, E., Salo, H., Laine, J., & Janz, J. 2018, *A&A*, 618, A34
- Leauthaud, A., Tinker, J., Bundy, K., et al. 2012, *ApJ*, 744, 159
- Lelli, F., McGaugh, S. S., & Schombert, J. M. 2016, *AJ*, 152, 157
- Leroy, A. K., Bolatto, A. D., Ostriker, E. C., et al. 2018, *ApJ*, 869, 126
- Lin, C. C., & Shu, F. H. 1964, *ApJ*, 140, 646
- Lin, C. C., & Shu, F. H. 1966, *PNAS*, 55, 229
- Lindblad, B. 1926, *Uppsala Meddelanden*, 11, 30
- Lindblad, B. 1927, *MNRAS*, 87, 420
- Lindblad, B. 1938, *ZA*, 15, 124
- Lindblad, B. 1941, *StoAn*, 13, 10.1
- Lindblad, B. 1963, *StoAn*, 5, 5
- Lindblad, B. 1964, *ApNr*, 9, 103
- Loeb, A., & Rasio, F. A. 1994, *ApJ*, 432, 52
- Longair, M. S. 1996, *Our Evolving Universe* (Cambridge: Cambridge Univ. Press)
- Longair, M. S. M. S. 2006, *The Cosmic Century: A History of Astrophysics and Cosmology* (Cambridge: Cambridge Univ. Press)
- Lu, Z., Mo, H. J., Lu, Y., et al. 2015, *MNRAS*, 450, 1604
- Lütticke, R., Dettmar, R.-J., & Pohlen, M. 2000a, *A&AS*, 145, 405
- Lütticke, R., Dettmar, R.-J., & Pohlen, M. 2000b, *A&A*, 362, 435
- Lynden-Bell, D. 1969, *Natur*, 223, 690
- Lynden-Bell, D., Faber, S. M., Burstein, D., et al. 1988, *ApJ*, 326, 19
- Mangum, J. G., Ginsburg, A. G., Henkel, C., et al. 2019, *ApJ*, 871, 170
- Martin, S., Muller, S., Henkel, C., et al. 2019, *A&A*, 624, A125
- Marx, G., & Szalay, A. S. 1972, in *Proc. "Neutrino 72"* Techninform 1, 123
- Mathewson, D. S., & Ford, V. L. 1996, *ApJS*, 107, 97
- Mathewson, D. S., Ford, V. L., & Buchhorn, M. 1992, *ApJS*, 81, 413
- Mayer, L., & Wadsley, J. 2004, *MNRAS*, 347, 277
- McGaugh, S. S., & Schombert, J. M. 2015, *ApJ*, 802, 18
- McGaugh, S. S., Schombert, J. M., Bothun, G. D., & de Blok, W. J. G. 2000, *ApJL*, 533, L99
- Mezcua, M. 2017, *IIMPD*, 26, 1730021
- Michikoshi, S., & Kokubo, E. 2014, *ApJ*, 787, 174
- Milgrom, M. 1983, *ApJ*, 270, 371
- Monaco, P., Salucci, P., & Danese, L. 2000, *MNRAS*, 311, 279
- Moster, B. P., Naab, T., & White, S. D. M. 2013, *MNRAS*, 428, 3121
- Moster, B. P., Naab, T., & White, S. D. M. 2018, *MNRAS*, 477, 1822
- Moster, B. P., Somerville, R. S., Maulbetsch, C., et al. 2010, *ApJ*, 710, 903
- Mould, J., Aaronson, M., & Huchra, J. 1980, *ApJ*, 238, 458
- Mowla, L., van der Wel, A., van Dokkum, P., & Miller, T. B. 2019, *ApJL*, 872, L13
- Mundell, C. G., Pedlar, A., Shone, D. L., & Robinson, A. 1999, *MNRAS*, 304, 481
- Mutlu-Pakdil, B., Seigar, M. S., & Davis, B. L. 2016, *ApJ*, 830, 117
- Mutlu-Pakdil, B., Seigar, M. S., Hewitt, I. B., et al. 2018, *MNRAS*, 474, 2594
- Navarro, J. F., Frenk, C. S., & White, S. D. M. 1996, *ApJ*, 462, 563
- Nemmen, R. S., Georganopoulos, M., Guiriec, S., et al. 2012, *Sci*, 338, 1445
- Oknyansky, V. L., Winkler, H., Tsygankov, S. S., et al. 2019, *MNRAS*, 483, 558
- Onken, C. A., Ferrarese, L., Merritt, D., et al. 2004, *ApJ*, 615, 645
- Onken, C. A., Valluri, M., Brown, J. S., et al. 2014, *ApJ*, 791, 37
- Oort, J. H. 1932, *BAN*, 6, 249
- Oort, J. H. 1940, *ApJ*, 91, 273
- Ostriker, J. P., & Peebles, P. J. E. 1973, *ApJ*, 186, 467
- Patsis, P. A., Skokos, C., & Athanassoula, E. 2002, *MNRAS*, 337, 578

- Paturel, G., Theureau, G., Bottinelli, L., et al. 2003, *A&A*, 412, 57
- Persic, M., & Salucci, P. 1988, *MNRAS*, 234, 131
- Peterson, B. M., Ferrarese, L., Gilbert, K. M., et al. 2004, *ApJ*, 613, 682
- Pizzella, A., Corsini, E. M., Dalla Bontà, E., et al. 2005, *ApJ*, 631, 785
- Planck Collaboration, Aghanim, N., Akrami, Y., et al. 2018, arXiv:1807.06209
- Posti, L., Nipoti, C., Stiavelli, M., & Ciotti, L. 2014, *MNRAS*, 440, 610
- Puech, M., Hammer, F., Flores, H., et al. 2010, *A&A*, 510, A68
- Puech, M., Hammer, F., Flores, H., et al. 2011, in IAU Symp. 277, Tracing the Ancestry of Galaxies, ed. C. Carignan, F. Combes, & K. C. Freeman, 138
- Reddick, R. M., Wechsler, R. H., Tinker, J. L., & Behroozi, P. S. 2013, *ApJ*, 771, 30
- Reynolds, J. H. 1925, *MNRAS*, 85, 1014
- Ringermacher, H. I., & Mead, L. R. 2009, *AJ*, 137, 4716
- Roberts, M. S., & Rots, A. H. 1973, *A&A*, 26, 483
- Roberts, W. W., Jr. 1975, *VA*, 19, 91
- Roberts, W. W., Jr., Roberts, M. S., & Shu, F. H. 1975, *ApJ*, 196, 381
- Rodríguez-Puebla, A., Primack, J. R., Avila-Reese, V., & Faber, S. M. 2017, *MNRAS*, 470, 651
- Rogstad, D. H., & Shostak, G. S. 1972, *ApJ*, 176, 315
- Romero-Gómez, M., Athanassoula, E., Masdemont, J. J., & García-Gómez, C. 2007, *A&A*, 472, 63
- Romero-Gómez, M., Masdemont, J. J., Athanassoula, E., & García-Gómez, C. 2006, *A&A*, 453, 39
- Rood, H. J. 1965, PhD thesis, Univ. Michigan
- Rubin, V. C., Ford, W. K., & Thonnard, N. J. 1978, *ApJL*, 225, L107
- Rubin, V. C., Ford, W. K., & Thonnard, N. J. 1980, *ApJ*, 238, 471
- Rubin, V. C., & Ford, W. K., Jr. 1970, *ApJ*, 159, 379
- Rubin, V. C., Thonnard, N., & Ford, W. K. J. 1977, *ApJL*, 217, L1
- Sabra, B. M., Akl, M. A., & Chahine, G. 2008, in IAU Symp. 245, Formation and Evolution of Galaxy Bulges, ed. M. Bureau, E. Athanassoula, & B. Barbu (Cambridge: Cambridge Univ. Press), 257
- Sabra, B. M., Saliba, C., Abi Akl, M., & Chahine, G. 2015, *ApJ*, 803, 5
- Saha, K., Graham, A. W., & Rodríguez-Herranz, I. 2018, *ApJ*, 852, 133
- Sahu, N., Graham, A. W., & Davis, B. L. 2019, arXiv:1903.04738
- Salo, H., & Laurikainen, E. 2017a, *ApJ*, 835, 252
- Salo, H., & Laurikainen, E. 2017b, AAS/Division of Dynamical Astronomy Meeting, 48, 303.02
- Salucci, P. 2019, *A&ARv*, 27, 2
- Sanders, R. H., & Lowinger, T. 1972, *AJ*, 77, 292
- Satyapal, S., Vega, D., Dudik, R. P., Abel, N. P., & Heckman, T. 2008, *ApJ*, 677, 926
- Satyapal, S., Vega, D., Heckman, T., O'Halloran, B., & Dudik, R. 2007, *ApJL*, 663, L9
- Savchenko, S. S., & Reshetnikov, V. P. 2011, *AstL*, 37, 817
- Savognan, G. A. D., Graham, A. W., Marconi, A., & Sani, E. 2016, *ApJ*, 817, 21
- Schawinski, K., Simmons, B. D., Urry, C. M., Treister, E., & Glikman, E. 2012, *MNRAS*, 425, L61
- Schawinski, K., Treister, E., Urry, C. M., et al. 2011, *ApJL*, 727, L31
- Schwarzschild, K. 1916, *Sitzungsberichte der Königlich Preußischen (Berlin: Akademie der Wissenschaften)*, 189
- Schwarzschild, M. 1954, *AJ*, 59, 273
- Seiden, P. E., & Gerola, H. 1979, *ApJ*, 233, 56
- Seigar, M. S. 2015, *Dark Matter in the Universe* (Bristol: IOP Publishing)
- Seigar, M. S., Block, D. L., & Puerari, I. 2004, in *Penetrating Bars Through Masks of Cosmic Dust, Astrophysics and Space Science Library*, Vol. 319, ed. D. L. Block et al. (Dordrecht: Kluwer Academic), 155
- Seigar, M. S., Block, D. L., Puerari, I., Chorney, N. E., & James, P. A. 2005, *MNRAS*, 359, 1065
- Seigar, M. S., Bullock, J. S., Barth, A. J., & Ho, L. C. 2006, *ApJ*, 645, 1012
- Seigar, M. S., Chorney, N. E., & James, P. A. 2003, *MNRAS*, 342, 1
- Seigar, M. S., Davis, B. L., Berrier, J., & Kenefick, D. 2014, *ApJ*, 795, 90
- Seigar, M. S., & James, P. A. 1998a, *MNRAS*, 299, 672
- Seigar, M. S., & James, P. A. 1998b, *MNRAS*, 299, 685
- Seigar, M. S., Kenefick, D., Kenefick, J., & Lacy, C. H. S. 2008, *ApJL*, 678, L93
- Sellwood, J. A. 2000, *Ap&SS*, 272, 31
- Sellwood, J. A. 2014, *RvMP*, 86, 1
- Sellwood, J. A., & Carlberg, R. G. 2014, *ApJ*, 785, 137
- Sellwood, J. A., & Evans, N. W. 2001, *ApJ*, 546, 176
- Sellwood, J. A., & Wilkinson, A. 1993, *RPPH*, 56, 173
- Seo, W.-Y., Kim, W.-T., Kwak, S., et al. 2019, *ApJ*, 872, 5
- Serra, P., Oosterloo, T., Cappellari, M., den Heijer, M., & Józsa, G. I. G. 2016, *MNRAS*, 460, 1382
- Shaw, M. A., Combes, F., Axon, D. J., & Wright, G. S. 1993, *A&A*, 273, 31
- Sheth, K., Elmegreen, D. M., Elmegreen, B. G., et al. 2008, *ApJ*, 675, 1141
- Shields, D. W., Boe, B., Pfountz, C., et al. 2015a, arXiv:1511.06365
- Shields, D. W., Boe, B., Pfountz, C., et al. 2015b, *Spirality: Spiral arm pitch angle measurement, Astrophysics Source Code Library*, ascl:1512.015
- Shlosman, I., Begelman, M. C., & Frank, J. 1990, *Natur*, 345, 679
- Shlosman, I., Frank, J., & Begelman, M. C. 1989, *Natur*, 338, 45
- Shu, F. H. 2016, *ARA&A*, 54, 667
- Silk, J., & Rees, M. J. 1998, *A&A*, 331, arXiv:astro-ph/9801013
- Simmons, B. D., Urry, C. M., Schawinski, K., Cardamone, C., & Glikman, E. 2012, *ApJ*, 761, 75
- Smith, S. 1936, *ApJ*, 83, 23
- Spitler, L. R., & Forbes, D. A. 2009, *MNRAS*, 392, L1
- Sun, A.-L., Greene, J. E., Impellizzeri, C. M. V., et al. 2013, *ApJ*, 778, 47
- Szalay, A. S., & Marx, G. 1976, *A&A*, 49, 437
- Takano, S., Nakajima, T., & Kohno, K. 2019, *PASJ*, in press (doi:10.1093/pasj/psz020)
- Tan, A., Xiao, M., Cui, X., et al. 2016, *PhRvL*, 117, 121303
- Taylor, E. N., Franx, M., Brinchmann, J., van der Wel, A., & van Dokkum, P. G. 2010, *ApJ*, 722, 1
- Thornley, M. D. 1996, *ApJL*, 469, L45
- Tiley, A. L., Bureau, M., Cortese, L., et al. 2019, *MNRAS*, 482, 2166
- Toomre, A. 1964, *ApJ*, 139, 1217
- Toomre, A. 1977, *ARA&A*, 15, 437
- Toomre, A. 1981, in *The Structure and Evolution of Normal Galaxies*, ed. S. M. Fall & D. Lynden-Bell (New York: Cambridge Univ. Press), 111
- Toomre, A., & Kalnajs, A. J. 1991, in *Dynamics of Disk Galaxies*, ed. B. Sundelius, 341
- Treister, E., Schawinski, K., Urry, C. M., & Simmons, B. D. 2012, *ApJL*, 758, L39
- Tremaine, S., Gebhardt, K., Bender, R., et al. 2002, *ApJ*, 574, 740
- Treuhardt, P., Seigar, M. S., Sierra, A. D., et al. 2012, *MNRAS*, 423, 3118
- Tsoutsis, P., Efthymiopoulos, C., & Voglis, N. 2008, *MNRAS*, 387, 1264
- Tsoutsis, P., Kalapotharakos, C., Efthymiopoulos, C., & Contopoulos, G. 2009, *A&A*, 495, 743
- Tully, R. B., & Fisher, J. R. 1977, *A&A*, 500, 105
- Valluri, M., Shen, J., Abbott, C., & Debattista, V. P. 2016, *ApJ*, 818, 141
- van den Bergh, S. 1960a, *ApJ*, 131, 215
- van den Bergh, S. 1960b, *ApJ*, 131, 558
- van den Bosch, F. C. 2000, *ApJ*, 530, 177
- van Dokkum, P. G., Leja, J., Nelson, E. J., et al. 2013, *ApJL*, 771, L35
- van Uitert, E., Hoekstra, H., Franx, M., et al. 2013, *A&A*, 549, A7
- van Wassenhove, S., Volonteri, M., Walker, M. G., & Gair, J. R. 2010, *MNRAS*, 408, 1139
- Vika, M., Driver, S. P., Graham, A. W., & Liske, J. 2009, *MNRAS*, 400, 1451
- Vogelsberger, M., Genel, S., Springel, V., et al. 2014, *MNRAS*, 444, 1518
- Voglis, N., Stavropoulos, I., & Kalapotharakos, C. 2006a, *MNRAS*, 372, 901
- Voglis, N., Tsoutsis, P., & Efthymiopoulos, C. 2006b, *MNRAS*, 373, 280
- Volonteri, M., Natarajan, P., & Gültekin, K. 2011, *ApJ*, 737, 50
- von der Pahlen, E. 1911, *AN*, 188, 249
- Walker, M. A. 1999, *MNRAS*, 308, 551
- Wang, L., Farrah, D., Oliver, S. J., et al. 2013, *MNRAS*, 431, 648
- Watson, A. M., Gallagher, J. S., III, Holtzman, J. A., et al. 1996, *AJ*, 112, 534
- Weiner, B. J., Willmer, C. N. A., Faber, S. M., et al. 2006, *ApJ*, 653, 1049
- Whitmore, B. C., & Kirshner, R. P. 1981, *ApJ*, 250, 43
- Whitmore, B. C., Kirshner, R. P., & Schechter, P. L. 1979, *ApJ*, 234, 68
- Williams, M. J., Bureau, M., & Cappellari, M. 2009, in *ASP Conf. Ser. 419, Galaxy Evolution: Emerging Insights and Future Challenges*, ed. S. Jogee et al. (San Francisco, CA: ASP), 167
- Xiao, T., Barth, A. J., Greene, J. E., et al. 2011, *ApJ*, 739, 28
- Yang, X., Mo, H. J., van den Bosch, F. C., Zhang, Y., & Han, J. 2012, *ApJ*, 752, 41
- Yu, S.-Y., & Ho, L. C. 2019, *ApJ*, 871, 194
- Yuan, T., Richard, J., Gupta, A., et al. 2017, *ApJ*, 850, 61
- Zahid, H. J., Geller, M. J., Fabricant, D. G., & Hwang, H. S. 2016, *ApJ*, 832, 203
- Zasov, A. V., Petrochenko, L. N., & Cherepashchuk, A. M. 2005, *ARep*, 49, 362
- Zhang, B., & Wyse, R. F. G. 2000, *MNRAS*, 313, 310
- Zubovas, K., & King, A. 2019, *MNRAS*, 484, 1829
- Zwicky, F. 1933, *AcHPH*, 6, 110
- Zwicky, F. 1937, *ApJ*, 86, 217